Synthesis and Characterization of Reduced Graphene Oxide Films

by

Fatimah Abdulbaqi Alussail

A thesis

presented to the University of Waterloo

in fulfillment of the

thesis requirement for the degree of

Master of Applied Science

in

Mechanical Engineering (Nanotechnology)

Waterloo, Ontario, Canada, 2015

AUTHOR'S DECLARATION

I hereby declare that I am the sole author of this thesis. This is a true copy of the thesis, including any required final revisions, as accepted by my examiners.

I understand that my thesis may be made electronically available to the public.

Abstract

The discovery of graphene properties in 2004 has replaced the need for indium titanium oxide on many applications. A large amount of research has focused on the advantages of using synthesis graphene as an inexpensive and clean process. In spite of a variety of synthesis methods which are able to produce high quality graphene sheet, Hummers method in synthesis graphene oxide has received the most attention due to its simplicity. This research illustrates the reduction method of graphene oxide and the restored conjugation structure of graphene sheet. Since using graphene oxide materials before reduction acts as an insulator, reduction process can improve electronic structure as well as electrical property. There are several methods used to fabricate reduced graphene oxide, including thermal reduction, chemical reduction, and photo reduction. Using one method is insufficient in producing a complete reduction of oxygen functional group. However, multi-step reduction is a new approach which relies on using two methods. Percentage of defect and surface morphology are factors that must be considered in preferring one method over another. Future research is needed to understand the mechanism of reduction, the increase and decrease defect ratio during reduction, the removable of oxygen atoms, and the rearrangement of carbon atoms.

Acknowledgements

First of all, I am thankful for Allah for all things.

Second, I am grateful to my parents, my husband, and my children for all of their support. They always encourage me and provide me with all that I need to complete my education.

I offer special thanks to my supervisor Professor Mustafa Yavuz for his guidance during my Master study. Professor Yavuz gave me opportunities to discuss experimental results during our meetings, and he provided me with knowledge.

I also want to thank Dr. Mehrdad Irannejad , who assisted me during research , and provide me with ideas.

Finally, I wish to thank King of Saudi Arabia Abdullah bin Abdulaziz Al Saud who gave me this opportunity by providing me with a full scholarship.

Table of Contents

List of Figures

List of Tables

List of abbreviations:

2D: two-dimensional

GO: graphene oxide

rGO: reduce graphene oxide

GIC: graphite intercalation compounds

CVD: chemical vapor deposition

AFM: atomic force microscopy

TEM: transmission electron microscopy

FTIR: Fourier transform infrared spectroscopy

UV-Visible: ultraviolet visible spectroscopy

SEM: scanning electron microscopy

XRD: X-ray diffraction

XPS: X-ray photoelectron microscopy

FET: field effect transistor

TE: transparent electrodes

ICs: integrated circuits

FLG: few layer graphene

MLG: multilayer graphene

LC: low concentration graphene oxide solution

HC: high concentration graphene oxide solution

Chapter 1: Introduction

1.1 Introduction to graphene

Single layer graphene , bilayer graphene , and few-layer graphene can be obtained from highly ordered pyrolytic graphite (HOPG) or synthetically from chemical derivative[1]. Graphene two-dimensional hexagonal structure is composed of Sp^2- hybridized bonded carbon atoms. Due to its exceptional carrier mobility, thermal conductivity, stiffness, and mechanical properties [2], graphene has gained much attention from researchers over the past decade. There are a variety of methods for graphene synthesis to satisfy the high demand on graphene. Two main approaches used to classify graphene synthesis methods are top-down and bottom-up. Fabrication methods such as mechanical exfoliation, epitaxial growth and reduction of graphene oxide exhibit both advantages and limitations [3]. While the mechanical exfoliation method of using Scotch-tape can produce high quality graphene film, this method is limited to study purposes rather than manufacturing processes due to the low yield [4]. Similarly, while epitaxial growth method can produce high quality graphene film with a lower level of defects, this method is considered expensive; furthermore, it needs high vacuum conditions and there is a difficulty in scale up [4]. Although chemical vapor deposition method is a good candidate for electronic application, further development in transfer film process from metal substrate to silicon substrate needs to be addressed [3]. In contrast, chemical exfoliation of graphite offers advantages over previous methods in terms of simplicity, low coast and scale up ability [3]. Chemical exfoliation using Hummers

method produces graphene oxide (GO) that includes a large number of functional groups. The presence of oxygen functional group destroys Sp^2 hybridization structure, produces defects, and increases the distance between stacked graphene layers [4]. However, utilizing multistep reduction methods can eliminate most of the oxygen functional groups [5]. Chemical reduction is widely used, but it leaves impurities. Similarly, thermal reduction at high temperature can eliminate oxygen group; however, this method results in loss of carbon atoms [6]. In a recent study, photo reduction of graphene oxide revealed advantages over other reduction methods as a green, clean approach [7]. Graphene oxide photo reduction is appropriate in specific applications such as photoluminescence and patterning [8]. Irradiation graphene oxide in solid state or solution by a different kind of irradiation has become a subject of study. The direct exposure of graphene oxide solution to laser or UV- light studied and published in many articles [8].

1.2 The history of graphene

The use of graphene dates back to between 1840 and 1859 when Schafhaeut developed the idea of graphite intercalation compound (GIC) by inserting dopants between graphene layers such as potassium sulfuric acid and nitric acid to assist the exfoliated graphite and to separate the stacked structures [9]. This process was further developed by adding a strong oxidation agent such as KCIO, by using sonication to provide chemical oxidation of the surface, and by giving graphene oxide (GO) materials that can be used in several applications. Between 1962 and 1969, Boehm adopted the notion of utilizing reduced graphene oxide (rGO) instead of using pristine graphene in the electronic application [9].

rGO was prepared via chemical reduction and thermal reduction of graphene oxide (GO). In 1970, Blakely successfully created a monolayer and multilayer carbon sheet on metal substrates such as Ni(100), Pd(100), and Pt(111) as a result of segregating carbon atoms on the surface [9]. In 1975 Van Bomme utilized ultrahigh vacuum (UHV) to sublime silicon from silicon carbide in a process called Epitaxial [9]. In 2004, graphene materials received scientific attention after Geim discovered mechanical exfoliation, or the "Scotch tape" approach, which could provide high quality graphene sheet with unusual properties [9].

1.3 Graphene definition and structure

Graphene is a two-dimensional carbon atom sheet in a honeycomb structure exfoliated from graphite. It has a hexagonal structure with two sub lattices bonded together with σ bonds. The π orbital in each carbon atom is partially filled below and above the plane [10, 11]. Graphene is a foundation for other important carbon allotropes, including 0D fullerene (C_{60}), 1D carbon nanotubes (CNTs), and 3D graphite (Figure1-1) [3].

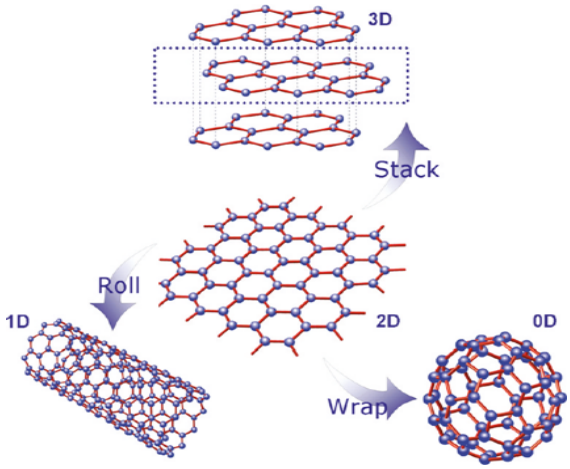

Figure 1-1: 2D Graphene is a foundation for other carbon allotropes [3].

Graphene can be obtained from natural graphite or synthetically generated from chemical derivative. Natural graphite, as shown in Figure 1-2(c) is a soft and good electrical conductor material, comprised of carbon atoms arranged in hexagonal rings. Graphene layers in natural graphite are stacked by loosely van der Waals bonds [1].

Graphene can be classified into three categories: monolayer, bilayer, and few-layer. Each category exhibits different electronic properties. Few-layer graphene has more than ten layers in a stacking arrangement such as rhombonedral stacking (ABCABC) or Bernal stacking (ABAB) Figure 1-2 (a). However, monolayer graphene does not exhibit a stacking structure; instead, it exists in rippled form [11]. Graphene can also be found in two types of edges: zigzag or armchair as is shown in Figure 1-2(b,d). Some graphene sheets exhibit both types of edge structures. In fact, magnetic and electronic properties can be tunneled by controlling the synthesis of one type of edge [11].

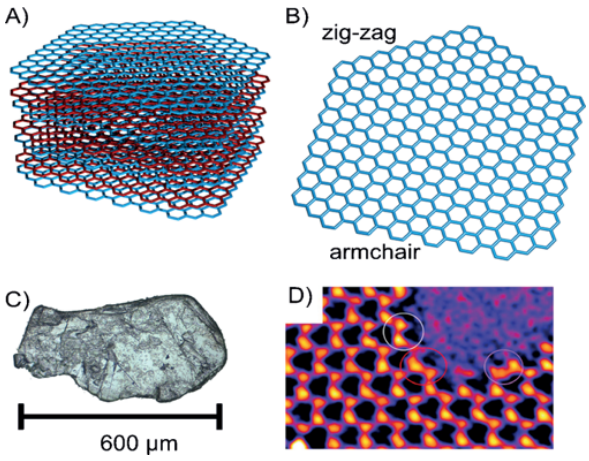

Figure 1-2: Schematic representation of (a) stacking of graphene layer; (b) graphene sheet with armchair and zig-zag edges; (c) photograph of nature graphite; and (d) high resolution transmission electron microscopy of armchair graphene edge [1].

1.4 Graphene properties and fabrication challenges

Since the discovery of graphene in 2004, the graphene field has progressed quickly due to its unusual properties in comparison to other carbon allotropes and functional materials. High electron mobility (2.5 x 105 cm^2 v^{-1} s^{-1}) at room temperature, high thermal conductivity above 3,000 Wmk^{-1}, Young's modulus of 1 TPa, high impermeability to gases, zero band gap, and high optical absorption are some of the exceptional properties of graphene [2].

However, producing graphene at a large scale is challenging in electronic industries. For example, the zero band gap of graphene has limited applications in the area of field effect transistor (FET). By developing a method of synthesizing graphene, band-gap tuning through a controlled number of layers, shapes, sizes, and defects could be a solution which would increase the applications of graphene in electronic industries [3].

1.5 Graphene application

1.5.1 Developing transparent electrodes (TEs) from graphene oxide (GO)

It has become necessary to find materials that can replace indium titanium oxide (ITO) as TE due to the high cost and limited resources of ITO. Graphene possesses high electron mobility, high flexibility, and unique mechanical properties which make it a promising candidate for ITO [3]. It is possible to produce GO film by a simple solution process at low cost. The GO film can be fabricated by spin coating technique, or vacuum filtration followed by reduction method [3]. Fabrication of reduced graphene oxide (rGO) occurs by chemical reduction or annealing improved film transparency and sheet resistivity performance. ITO offers high

transparency of 90% with low sheet resistivity of 10-30 Ω/sq [3]. The optical transparency of rGO films can be increased as high as 96% by doping gold chloride [3].

1.5.2 Fabricating field effect transistor (FET) from graphene oxide solution

Gold (AU) is the current material that is used as source and drain electrodes in FET. However, fabrication of source, drain, and gate from graphene oxide solution offer better performance in terms of mobility, sheet resistivity, and ON/OFF ratio. Figure 1-3 illustrates FET fabricated graphene film on flexible substrate using pentacene as channel materials. The performance of FET made from graphene materials shows a better ON/OFF ratio of 10^6, and electron mobility of $0.020 cm^2/(v.s)$ compared with gold FET [3].

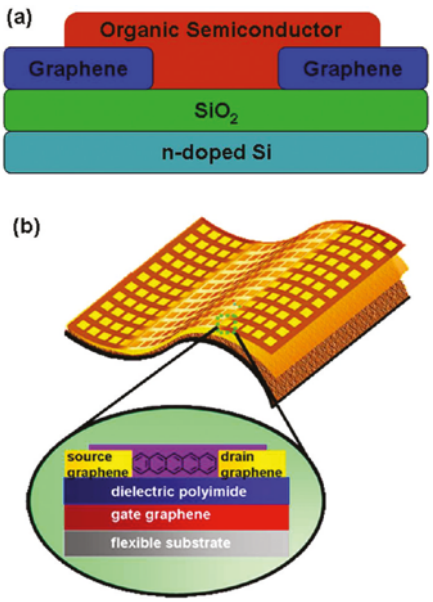

Figure 1-3: FET showing source, drain, and gate made from graphene [3]

1.5.3 Organic photovoltaic (OPV) and light emitting diode from graphene transparent electrodes

Figure 1-4 (a) shows a bilayer organic photovoltaic device with graphene oxide electrodes. The transmittance of graphene film is 95%; however, the sheet resistivity is higher than 100 kΩ/sq [3]. The power conversion efficiency (PCE) is low at approximately 0.4%. Fabricating of bulk hetero junction (BHJ) structure for organic photovoltaic devices could increase the PCE to a maximum of 1.01% by reducing graphene oxide, as shown in Figure 1-4(b). In organic light emit diode, graphene replaces ITO as anode electrode, as shown in Figure 1-4(c). The device shows a luminance of 300 cd /m^2, which is similar to ITO; however, the sheet resistivity of graphene film is as large as 800Ω/sq [3].

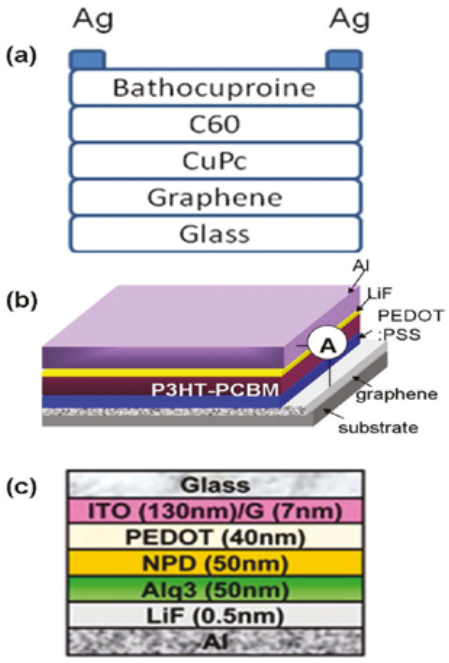

Figure 1-4: (a) bilayer organic photovoltaic; (b) bulk hetero junction; and (c) light emitting diode which replaces ITO with graphene [3].

1.6 Thesis overview

In this work, I attempted to study the effect of direct low thermal annealing and deep UV exposure of graphene oxide film on reduction mechanism. This experimental work includes several steps. In the first step, graphene oxide films were fabricated using commercial aqueous graphene oxide solutions and a technique of spin coating followed by annealing at different low temperatures and baking times. Raman spectroscopy and atomic force microscopy were carried out to study the degree of defects, disorders, and surface morphology of samples, respectively. In the second step, different concentrations of graphene oxide solution were mixed with ethanol. Dispersion of graphene oxide in ethanol were studied in terms of transmittance, defect, surface morphology, and carbon/oxygen ratio using different spectroscopic techniques. In the last steps, the graphene oxide films were exposed with deep UV light and the effects of exposure on the material properties of graphene oxide film were investigated.

1.7 Conclusion

Graphene is the most promising material in the nano material field due to it is unique properties. The production of high quality graphene at low cost, large size, and with a reproducible method remains a challenge. Different applications require different graphene qualities, since the presence of defects, structure disorders, wrinkles, and grain boundaries can reduce electron carrier mobility. Among a variety of graphene synthesis methods,

graphene oxide solution process can resolve scalability limitations, and reduce manufacturing coast.

Chapter 2: Graphene Characterization Tools

2.1 Introduction

This chapter reviews some spectroscopic and characterization techniques of graphene and graphene oxide sheets. The Raman spectroscopy, which is the most powerful technique in graphene and graphene oxide material characterization, was employed to precisely measure defects, structure disorders, and number of layers. In addition to Raman spectroscopy, atomic force microscopy (AFM) and scanning electron microscopy (SEM) were used to detect film thickness, roughness, and number of layers as well as size of the graphene oxide flakes. The electronics absorption and molecular vibration frequencies of graphene oxide sheets can be studied using the UV-VIS and Fourier transform infrared spectroscopy, respectively. The X-ray photoelectron spectroscopy was used to study the carbon/oxygen atomic ratio and molecular binding energy of chemical composition.

2.2 Raman spectroscopy

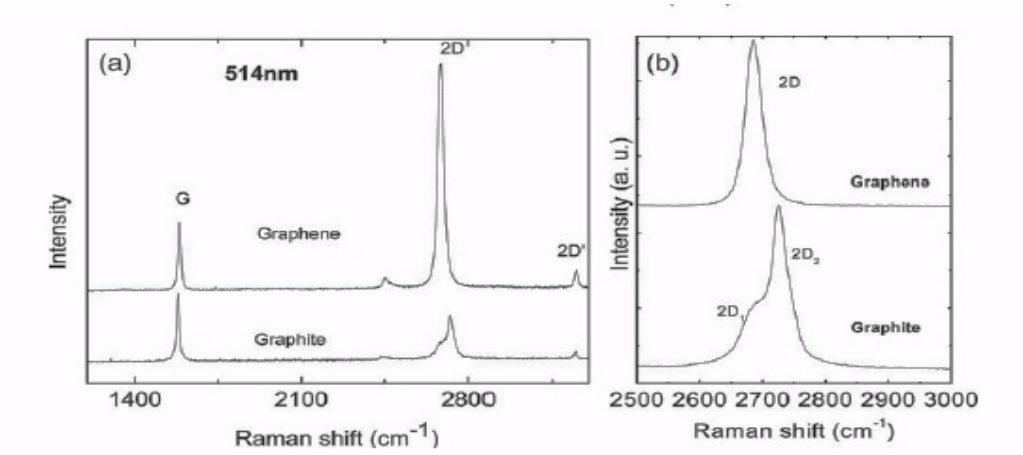

Figure 2-1: (a) Comparison of Raman spectra of graphite and graphene; (b) Comparison of 2D peaks in graphene and graphite [12].

Raman spectroscopy is a powerful technique in materials research. Material properties can be characterized by using Raman spectroscopy without damaging the sample. Information such as atomic structure, number of layers, type of edge, type of disorder, and functional groups of a graphene/graphene oxide sheet can be precisely determined from its Raman spectrum. These properties can be studied by the Raman shift, peak's shape, position, and intensity [13]. Figure 2-1(a) shows the recorded Raman spectrum of graphene and graphite at excitation wavelength of 514 nm. As can be seen, the main two features were recorded at wavenumber of 1580cm^{-1} and 2700cm^{-1} which was assigned to the G band and the 2D band, respectively. The number of graphene layers can be determined from 2D band position and its broadness (FWHM). As it is clear from Figure 2-1(b), the shape of the 2D band is different in graphite compared to graphene. The 2D band in graphite consists of two peaks,

while 2D band in graphene shows only one sharp peak. This is due to the smaller number of layers in graphene and the different mechanism of electron-phonon scattering relative to graphite [14].

In contrast, Raman spectrum of any graphene oxide in the range of 1100cm^{-1} to 3000cm^{-1} includes three major peaks at wavenumbers of 1300cm^{-1}, 1580cm^{-1}, and 2680 cm^{-1}, which is named as D, G, and 2D respectively as shown in Figure 2-2. The presence of D band indicates a defect in the graphene sheet. However, the presence of G band in 1580 cm^{-1} is due to scattering in E_{2g} mode [13]. In some cases, G band could have a blue shift from 1580 cm^{-1} in graphite to more than 1593cm^{-1} in graphene oxide, which is due to the functionalization of graphene [14]. The appearance of 2D band in Raman spectra is clear evidence of graphene existence. For example, a single layer of graphene was identified in the area of 2685cm^{-1} and FWHM of 25cm^{-1}. The intensity ratio of D band and G band provides information related to structural defects in a graphene sheet. For example, the ratio of ID/IG increases after annealing due to loss of carbon atoms [14].

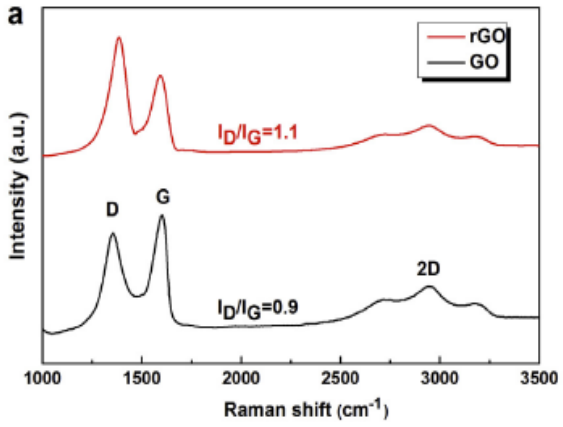

Figure 2-2: Rama spectra of graphene oxide and reduced graphene oxide [15]

2.3 Atomic force microscopy

Atomic force microscopy (AFM) is used in characterizing a variety of specimens such as biological, semi-conductor, and polymer samples. AFM can provide information regarding surface morphology in micro-and nano scale [16]

AFM is utilized to calculate intermolecular forces as well as scanning electron microscopy (SEM) and transmission electron microscopy (TEM). A common AFM system (Figure2-3) includes a piezoelectric (PZT) actuator, a sharp tip which is placed in the top of the cantilever probe, a sensitive photo detector, and a monochromatic light. The principle of AFM employs a tip that scans the surface of the sample at a constant height and force that is provided by PZT. The end-point of the laser beam impinges the cantilever, then deflects the light to the sensitive photo detector. The different light intensities and phases measured by photo detractor provide information about the surface [16].

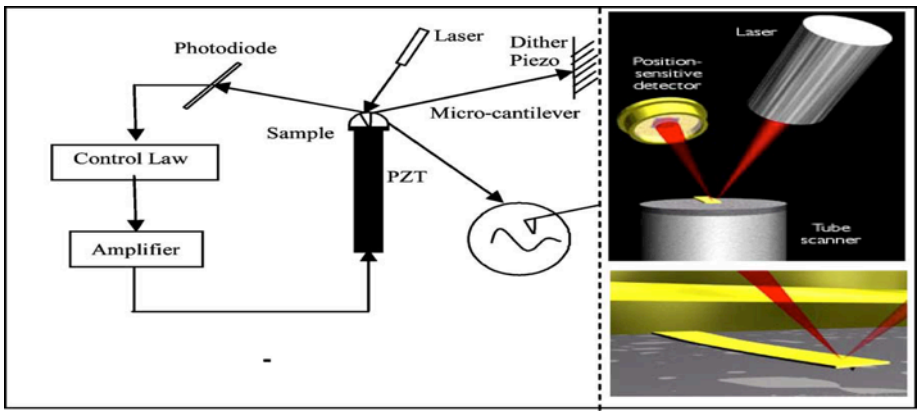

Figure 2-3: Atomic force microscopy operation [16]

The AFM has three open-loop modes: contact mode, non-contact mode, and tapping mode (Figure 2-4). In contact mode the tip is in mechanical contact with the sample, whereas in non-contact mode the cantilever oscillates near the surface of the sample. In tapping mode the contact and non-contact methods are employed so that the cantilever tip touches the sample and oscillates in resonance frequency [16].

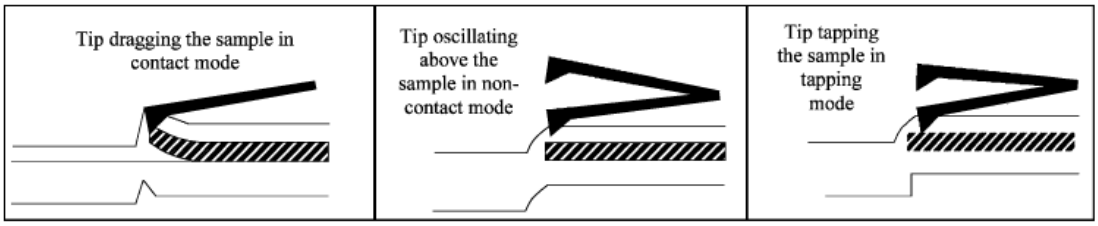

Figure 2-4: Schematic explanation of contact mode, noncontact mode, and tapping mode of AFM [16]

2.4 Scanning electron microscopy

Scanning electron microscopy (SEM) is a powerful tool that is utilized in characterizing sample morphology such as grain size, particle size, and surface structure.

In 1890 researchers discovered that electrons can deflect after impinging the sample and in presence of magnetic field [17]. Electron microscopy replaces the light source in traditional microscopy with a high energy electron beam source. However, the resolution is restricted to source wavelength. The formation of SEM image is dependent on the amount of signals produced as a result of interaction between electron beam and specimen. This interaction can be classified into two categories: elastic interaction and inelastic interaction. Elastic interaction results form deflecting electrons without loss of energy. For example,

backscattered electrons (BSEs) are elastic scattered at a 90^{o} angle. In contrast, inelastic scattering occurs in many signals, which causes energy to transfer from electrons to atoms. As a result excitation of electrons occurs and generates secondary electrons (SEs). In addition to secondary electrons and backscattering electrons which are used to form the image, there is another signal used to provide chemical information such as X-ray, Auger electrons, and cathode luminescence (Figure 2-6).

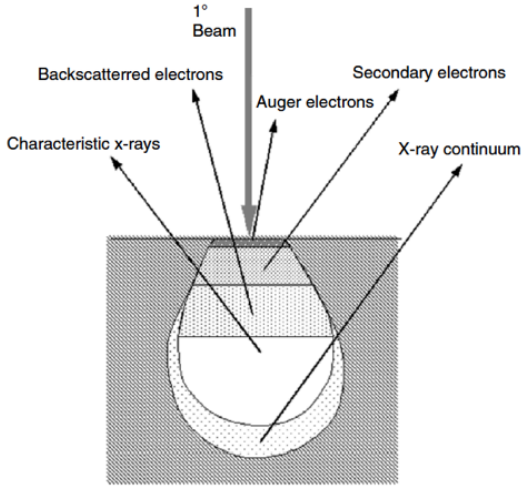

Figure 2-5: Signals generated as a result of electron beam interaction with sample; as well, information is given from the region that the signal can detect [17].

The most important signal resulting from the electron beam interacting with the specimen is secondary electrons. Inelastic scattering causes removal of electrons from outer shell atoms and ionization atoms. Secondary electrons escape from area of nanometer and have lower energy from 3-5 eV. Secondary electrons are used in SEM to visualize surface roughness and texture. The quality of image depends on how many secondary electrons reach the detector [17].

2.5 UV – VIS spectroscopy

UV-VIS spectroscopy is carried out to study the electronic absorption of graphene oxide and reduced graphene oxide films. Figure (2-11) shows the UV-VIS spectrum of Graphene oxide dispersed in a mixture of water and ethanol and irradiated for 35.3 kGy with γ- ray. As evident in Figure 2-11, the colour of the GO solution changes from yellow to black as a result of irradiation and therefore the reduction process. As is clear from this figure, the UV-VIS spectrum has two absorption peaks at wavelengths of 230nm and 290nm before exposure to γ-ray, which are assigned to show two peaks in wavelengths of C-C and C=O molecular absorption, respectively [18]. After exposure the C=O peak disappears, and C-C peak is recorded at wavelength of 270nm [18].

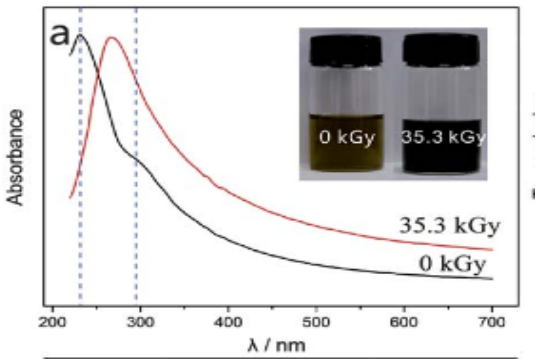

Figure 2-6: UV-Vis spectra of graphene oxide before and after γ- ray irradiation [18]

2.6 Fourier transform infrared spectroscopy

Fourier transform infrared (FTIR) spectroscopy is widely used to provide information on the molecular structure of different specimens. The spectroscopy range can be categorized into three categories: near infrared (NIR) (12800 to 4000 cm^{-1}), mid infrared (MIR) (4000 to 200 cm^{-1}), and far infrared (FIR) (50 to 1000 cm^{-1}) [19]. However, the most common region is MIR (4000 to 400cm^{-1}) due to the fact that the molecular vibration of most organic compounds were laid in this range. FTIR spectroscopy offers advantages over other techniques by its capability to analyze a diversity of samples in liquid, gas, or solid. Moreover, the developed FTIR spectrometer provides recorded absorption/transmission spectrum with high accuracy and high resolution. The infrared spectroscopy relies on the absorption of specific frequency by molecular bond which is resonant frequency of molecular vibration of that bond. The absorption energy is determined by the shape of molecular bonds (e.g. stretching, and bending), its surface potential energy, the mass of the atoms, and molecular bonding strength [19]. Figure 2-12 shows a typical transmittance spectrum of GO and rGO in the infrared range that was recorded by FTIR spectrometer. As can be seen from this figure, several molecular vibration frequencies are recorded in GO specimen, which indicates that GO specimen has hydroxyl (-OH), carbonyl (-C=O), and epoxy groups (C-O-C). After the reduction process these functional groups were reduced significantly [15].

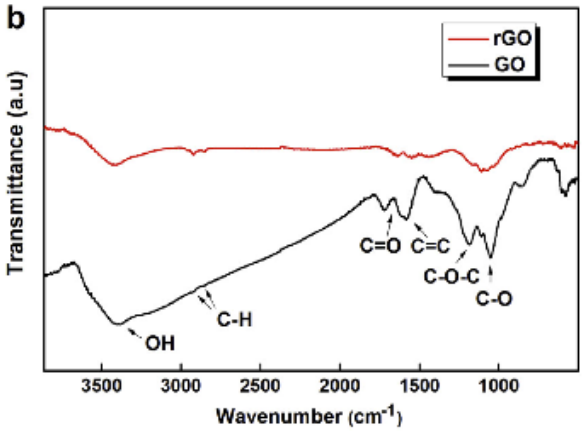

Figure 2-7: Recorded FTIR spectrum of graphene oxide (GO) and reduced graphene oxide (rGO) [15]

2.7 X-ray photoelectron spectroscopy

X-ray photoelectron spectroscopy (XPS) is a powerful technique that is used to analyze surface chemical composition. In this technique the specimen surface is irradiated by X-ray beam that penetrates deeply inside the specimen. Consequently, a number of electrons eject and their kinetic energy is measured. In fact, X-ray photoelectron spectroscopy is widely utilized in material characterization research such as graphene oxide characterization to assess the efficiency of reduction method by calculating the carbon to oxygen atomic ratio and the binding energy of carbon functional groups [5]. Figure 2-13 shows the XPS spectrum of the graphene oxide film before and after the reduction process. As shown in Figure 2-13(a), several functional groups at different binding energies such as C-C (~284.6 eV), C-O (~ 286.2 eV), C=O (~287.8 eV), and (O-C-O (289.1 eV) are recorded. Whereas in the reduced graphene oxide film, the intensity and therefore their atomic ration are significantly

reduced, which is followed by significant increases in the C-C intensity as is clear from Figure 2-13(b) [5].

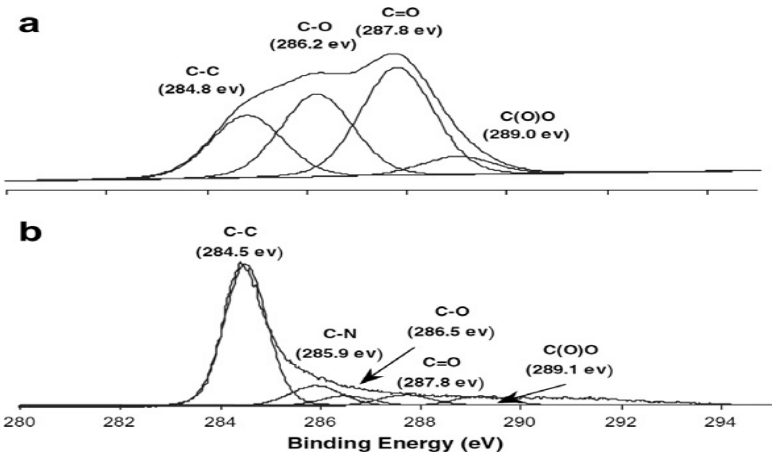

Figure 2-8: XPS spectra (a) graphene oxide film; (b) reduced graphene oxide film [5]

2.8 Conclusion

Different spectroscopic techniques are important in graphene and graphene oxide characterization, including Raman spectroscopy, X-ray photoluminescence spectroscopy, UV-VIS, and infrared spectroscopy, AFM and SEM are reviewed shortly.

It has been shown that the Raman spectroscopy is the most important technique in chemical analysis due to its sensitivity and accuracy. Moreover, atomic force microscopy and scanning electron microscopy provide useful information about surface morphology of the graphene oxide films such as flake shape, film thickness, and surface roughness. UV-VIS, Fourier transform infrared, and X-ray photoelectron spectroscopy are utilized to study electronic absorption, molecular absorption, carbon/oxygen atomic ratio, and binding energy of the graphene oxide specimens before and after reduction process.

Chapter 3: Graphene Synthesis Methods

3.1 Introduction

Since the discovery of graphene in 2004, enormous efforts has been established to produce high quality graphene sheet. Graphene synthesis methods are classified into two categories: bottom-up approach and top-down approach. A variety of synthesis methods provide a wide range of choices in terms of quality. Whether one method is preferable to another depends on application. While bottom-up approach provides a defect-free graphene sheet, this approach is considered to be expensive and limited in scale up. In contrast, top-down approach resolves the price and size issues, but the quality of graphene sheet needs further improvement [11].

3.2 Bottom-up method

Bottom-up method is utilized to produce graphene sheet from decomposition of carbon resources at high temperature. Using chemical derivative as a source for carbon atoms rather than graphite material is preferable to obtain pure graphene sheet that is free of defect. The epitaxial growth and chemical vapor deposition (CVD) are some examples of this method [11].

3.2.1 Epitaxial growth

Epitaxial growth is the growth of crystalline materials at the top of insulator substrate.

The mechanism of this technique depends on raising the temperature of SiC substrate under ultra high vacuum conditions. Due to the fact that there is a difference in vapor pressure between silicon and carbon, silicon atoms tend to dissociate from the surface and rise up, while carbon atoms form a graphene sheet Figure 3-1(a) [20].

Graphene sheet growth on hexagonal SiC (0001) has two faces. Si-terminated (0001) face is utilized for growing few-layer graphene (FLG). However, C-terminated (0001') face is utilized for growing multilayer graphene (MLG) Figure 3-1(b) [20].

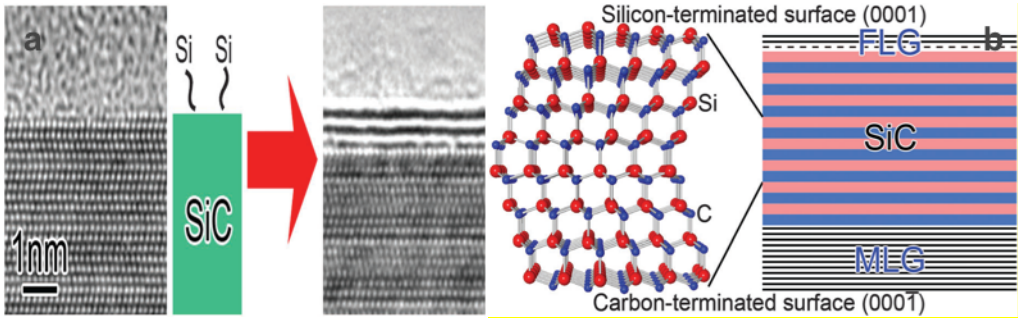

Figure 3-1: (a) Basic mechanism of epitaxial growth in Sic; (b) Graphene growth on Sic substrate in both carbon- and silicon-terminated faces [20].

Graphene film growth on Si-face exhibits a beneficial approach in controlling the film thickness in addition to controlling the number of layers. The mechanism starts with step edge nucleation then follows layer by layer. By utilizing high-resolution transmission electron microscopy (HRTEM), Figure 3-2(a) reveals buffer layers which are carbon atoms arranged periodically followed by graphene layers. Tuning growth temperature is used to specify the number of layers.

In the case of graphene film growth on C-face, there is no homogenous multilayer graphene growth. Due to the fact that nucleates separate everywhere, the mechanism of growth does not follow the layer-by-layer method. Moreover, buffer layer does not appearing in C- face growth Figure 3-2(b) [20].

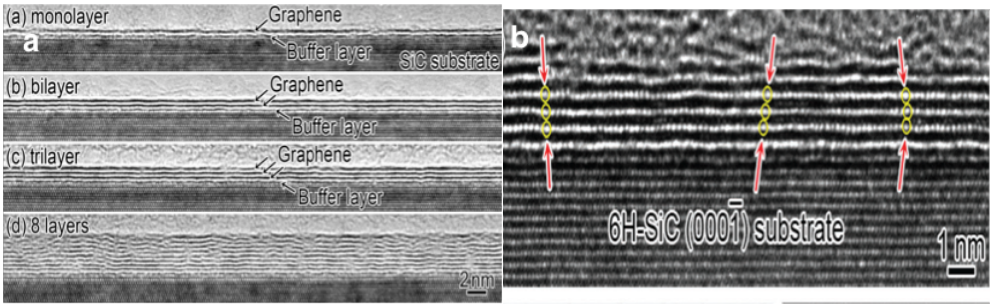

Figure 3-2: (a) HRTEM image represents the growth of graphene monolayer-bilayer-trilayer-8-layer and the periodic carbon atoms in buffer layer; (b) TEM image for graphene growth on c-face [20]

3.2.2 Chemical vapor deposition (CVD)

The growth of graphene film using CVD technique was reported in 2009 for first time [21]. In this technique, the graphene film is grown on the metal substrate such as nickel (Ni) or copper (Cu) and is then transferred to different substrates like Si or polymer substrate. Choosing catalytic metal for graphene film growth can be critical due to the fact that metal can effect graphene sheet quality. Graphene growth using CVD includes three main steps. In the first step, metal substrate is annealed at high temperatures as high as 1000 ^{o}C in Ar/H_2 atmosphere to increase grain size. In the second step, the mixture of H_2/CH_4 strikes the substrate, whereas carbon atoms in methane dissolve in Ni substrate. During the cooling process, carbon atoms rise up to form graphene sheet as it is shown schematically in Figure

3-3. There are several factors that affect the film quality such as cooling temperature rate, substrate surface microstructure and growth rate [21].

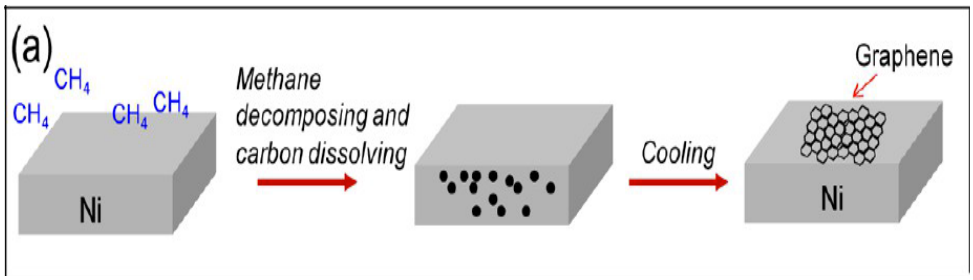

Figure 3-3: Graphene film deposition on the Ni substrate through chemical vapor deposition [21]

By using different kind of metals, Cu was shown to be the best option to replace Ni due to its cost-effectiveness, ability to control the graphene growth mechanism, and ability to facilitate the transfer process to the different substrates.

The mechanism of growing graphene film on the Cu substrate can be summarized in few steps. First, in the furnace, Cu foil is annealed to 1000^{o}C in the presence of hydrogen gas. Second, a mixture of methane and hydrogen is introduced to the chamber. Finally, the system cools down after the formation of the graphene layer [21].

Optical microscopy and Raman spectroscopy are utilized to compare graphene growth in Cu and Ni Figure 3-4. Optical image shows uniform monolayer graphene in the case of polycrystalline Cu substrate while polycrystalline Ni reveals multilayers of graphene. Raman spectroscopy further confirms this result. The amount of carbon atoms that dissolved in Cu substrate is low compared to Ni substrate. This fact is attributed to the formation of a segregation process in graphene film growth in Ni Figure 3-4 [21].

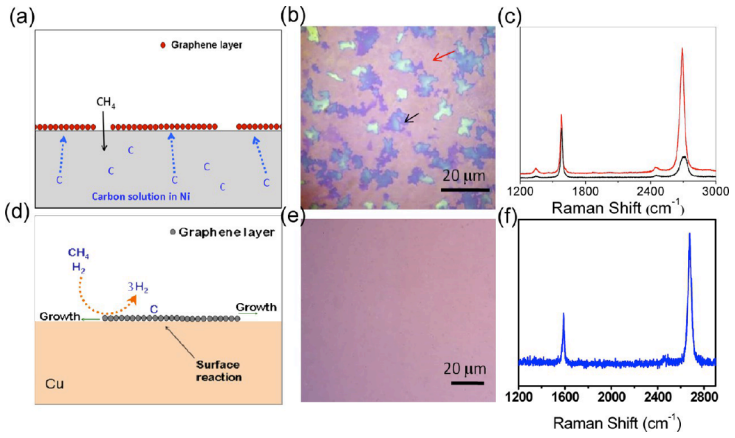

Figure 3-4: (a)(d) graphene formation on Ni/Cu; (b)(e) optical image of graphene on SiO_2/Si substrate from Ni and Cu, respectively; (c)(f) Raman spectroscopy of graphene on Ni and Cu, respectively [21]

Finally, graphene sheet is transferred to arbitrary substrate, as shown in Figure 3-5. First, graphene film is coated by polymethyi methacrylate (PMMA). Next, graphene film is annealed at high temperature to evaporate the solvent. After that, metal is etched and removed from graphene film. Finally, PMMA in the top of graphene transferred to substrate and removed by acetone.

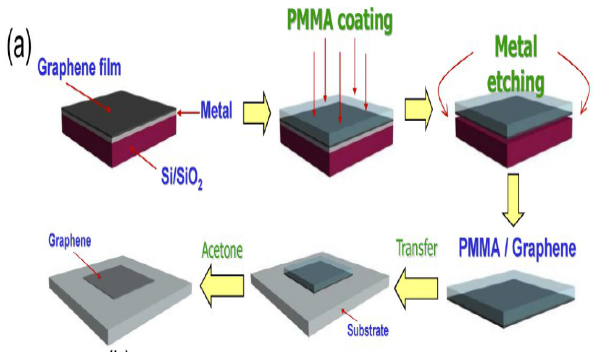

Figure 3-5: Schematic diagram for graphene transfer process to substrate [21].

3.3 Top-down method

The mechanism of the top-down method relies on separating the single graphene sheet from graphite by overcoming the weak van der Waals force. Graphite is used as a sources for carbon atoms. The main disadvantage of this approach is that layers may re-agglomerate after being exfoliated; also, graphene sheet could be damaged in the separation process. There are several top-down methods such as mechanical cleavage, electrochemical exfoliation, exfoliation of graphene intercalation compound, and exfoliation of graphene oxide (Hummers method) [11].

3.3.1 Mechanical cleavage

Scotch tape or peel off method produces high quality graphene sheet. Graphene sheet is separated from graphite by using adhesive tape. After that, the sheet is transferred to Sio_2/Si substrate. Use of optical microscopy and atomic force microscopy can identify the number of

layers. This technique is appropriate for studying graphene quality and properties rather than for manufacturing, due to the low yield [11].

Another mechanical cleavage method uses ultra sharp single crystal diamond wedge in the presence of ultrasonic oscillation. Figure 3-6 shows the experimental set-up by cutting high ordered pyrolytic graphite (HOPG) in size of 1 x 1 x 2mm. After that, epofix is utilized to staple and organize HOPG materials as a pyramid. Finally, sections are made in the sample by using ultra-sharp diamond wedge enhanced by ultrasonic oscillation system. Cleaved layers are transferred to copper substrate or Si/Sio_2 substrate to perform characterization [22].

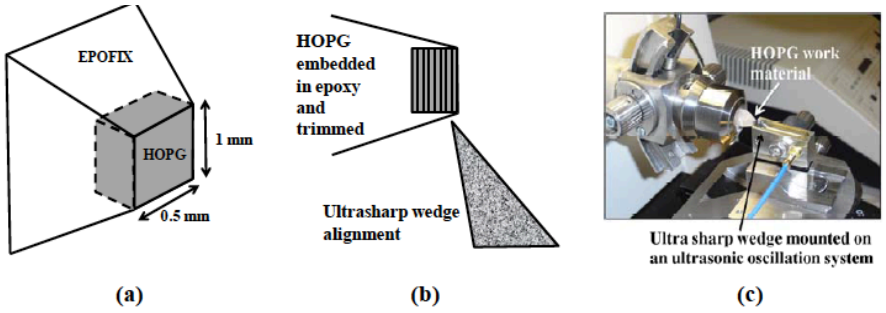

Figure 3-6: Mechanical method in synthesis graphene by ultra-sharp wedge (a) Epofix is utilized to embedded HOPG; (b) Wedge alignment; (c) Actual system wedge and ultrasonic oscillation [22]

3.3.2 Electrochemical exfoliation

Electrochemical exfoliation is another top-down method of producing graphene sheet from scarified graphite materials in one step. Figure 3-7 illustrates the process of electrochemical exfoliation of high order pyrolytic graphite. Figure 3-7(a) shows the electrolyte solution consisting of sulfuric acid H_2 SO_4 4.8g diluted in 100ml water. Graphite materials are employed as electrode and platinum (Pt) is a grounded electrode connected to DC bias. The

image in Figure 3-7(b) shows the HOPG materials before exfoliation after applying low bias +1v which assist SO_4 ions to be intercalated with graphite [23].

After that, high bias +10 v is applied to dissociate the material into small layers. In the final stage, graphene layers are collected by filtering the solution. The layers are then re-dispersed in dimethyl-formamide (DMF) solution [23].

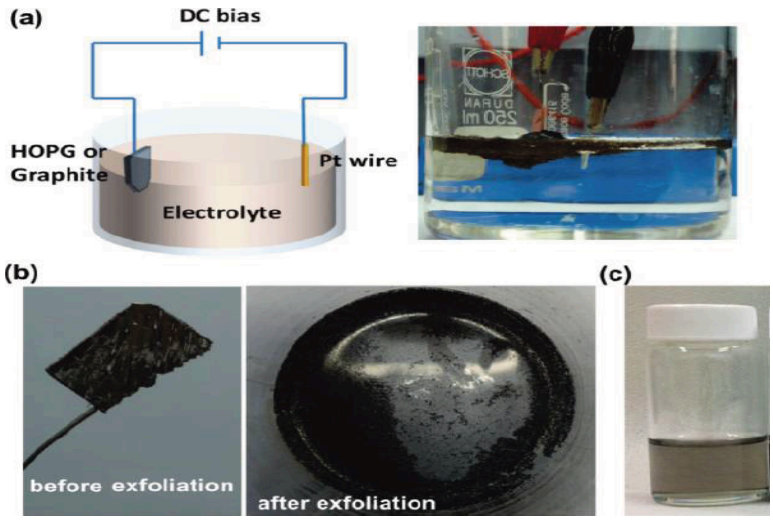

Figure 3-7: (a) Electrochemical exfoliation process; (b) Graphite before and after applying the bias; (c) After collecting graphene layers and dispersing them in DMF solution [23]

3.3.3 Exfoliation of graphene intercalation compounds (GIC)

Solvent assistance and thermal exfoliation are two methods used to produce graphene from GIC. Utilizing solvent can assist in expansion and exfoliation of graphene layers in the presence of sonication. This process relies on the idea of simulating gas as a result of interaction with solvent which aids exfoliation [11].

For instance, lithium intercalation with graphite materials cause expanded graphite sheet in the presence of water and sonication. Hydrogen gas was formed to aid the exfoliation Figure 3-8 [11].

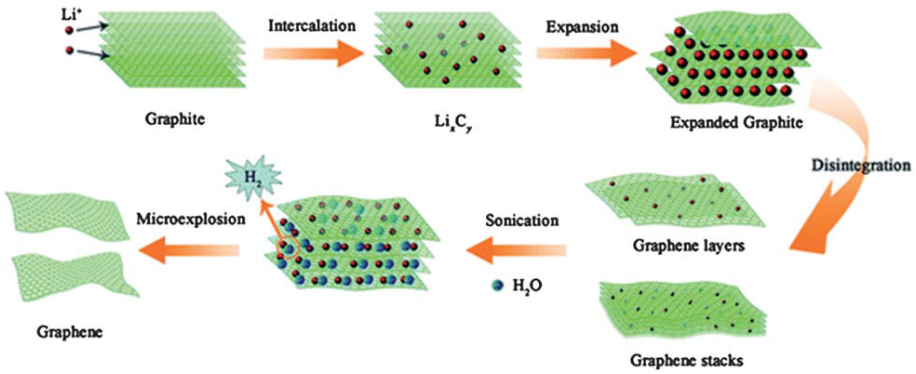

Figure 3-8: IGC of graphite with lithium compounds [11]

Thermal exfoliation of graphite first began in 1916; however, this approach did not develop until the fabrication of foils to gasket in the 1960s. This method relies on heating GIC which causes decomposition of intercalation component and the release of gases that aid in the exfoliation that separates the graphene sheet [11].

3.3.4 Exfoliation of graphene oxide (Hummers method)

Hummers method of synthesizing graphene oxide has received the most attention due to its simplicity and efficiency. The graphene oxide structure is illustrated by Lerf-Klinowski in Figure 3-9. Graphene oxide layer in Lerf-Klinowski's illustration shows hydroxyl and epoxy group inside the sheet; however, carbonyl and carboxylic are on the edge of the graphene oxide sheet [11].

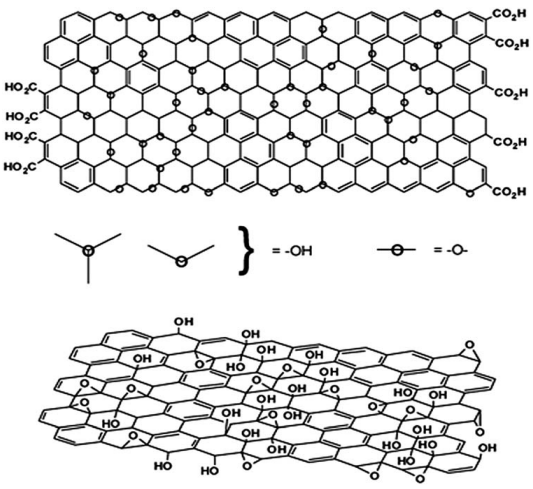

Figure 3-9: Lerf-Klinowski model illustrating the structure of graphene oxide [11]

Graphene oxide has received intensive research compared to other graphene synthesis methods. Graphene oxide provides materials that are inexpensive, have high yield, and are highly hydrophilic. Graphene oxide contains carbon atoms and oxygen groups which destroy the prosperity of the graphene oxide sheet and contribute to increasing the interlayer distance. Hydroxyl and epoxy groups destroy localized π electrons which contribute to decreasing carrier mobility. However, there is a wide range of techniques that can be utilized to remove oxygen group and restore the property of graphene oxide sheet in a process called reduced graphene oxide (rGO) [5].

There are several methods that can be utilized to assess the effect of reduction process on graphene oxide sheet. Visual characterization of graphene oxide solution and film can determine the efficiency of the reduction process, since carrier mobility and concentration improves after reduction. For example, in the case of observing the chemical reduction of graphene oxide solution, it is obvious that the colour changes from yellow-brown to black as

a result of the polar functionality changing to a lower level in the surface. In addition to observing the colour, optical microscopy can reveal a clear difference between GO/rGO sheets on SiO_2/Si substrate. Graphene oxide film shows a lower contrast with substrate which is clear evidence of being an insulator; however, rGO shows improvement in contrast with substrate [5].

3.4 Reduce grapehene oxide methods

3.4.1 Thermal reduction

Reduced graphene oxide has been a significant topic of research. One approach is thermal reduction of graphite oxide at elevated temperature. Increasing the temperature to more than 2000^{o}C can cause decomposition for oxygen atoms as well as exfoliated graphite oxide. Disadvantages of using this method include small size graphene sheet and defects. Small size sheet is mainly attributed to carbon atoms being removed from the graphene sheet during decomposition of oxygen atoms. Due to the loss of mass and structure defect during thermal exfoliation of graphite oxide, electrical conductivity decreases. However, large graphene sheet can be produced by exfoliate graphene oxide in liquid phase. The mechanism first makes film or powder from graphene oxide solution, and is then annealed.

Elevated temperature is needed to achieve good graphene oxide structure. For example, GO film annealed at 500^{o}C revealed lower electrical conductivity, and the films annealed at 1100^{o}C revealed higher electrical conductivity. The drawback of this technique is the large energy consumption and the slow process to avoid expansion of the film [5].

3.4.2 Photo reduction by UV-Light

Another beneficial approach in reduced graphene oxide is photo reduction by using UV irradiation to reduced graphene oxide sheet. Exposing graphene oxide solution to UV irradiation causes formation of graphene in liquid phase. Observing the absorption peaks for graphene oxide before and after UV irradiation using UV-visible spectra can monitor the process. In Figure 3-10, the spectra revealed redshift of peaks from 230nm (C-C) to 260nm, which is a clear indication of graphene formation. This process requires lengthy exposure for approximately 24 hrs. The colour is observed to changing from light to dark brown [7].

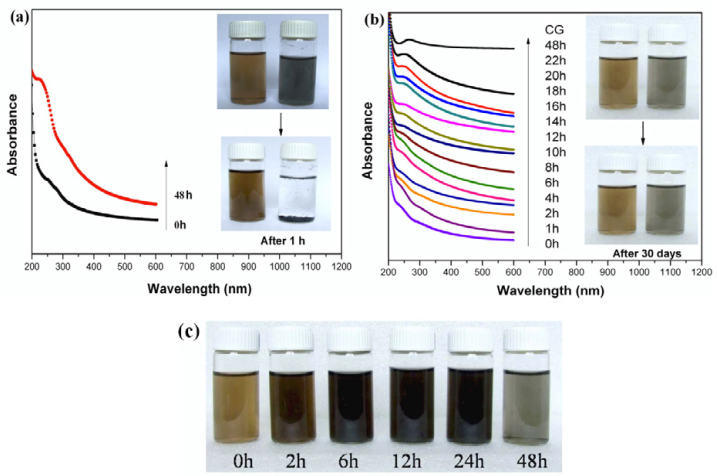

Figure 3-10: (a)UV-visible of GO before and after exposure to UV irradiation;(b) PolyvinyI Pyrrolidone (PVP) is used to enhance the process of reduced graphene oxide; (c) Colour change after UV irradiation [7]

3.4.3 Reduced graphene oxide via laser

Graphene oxide materials are not conductive. Reduced graphene oxide by laser exposure can remove oxygen components and improve electrical conductivity of materials. Exposure of graphene oxide solution to pulsed laser can quickly reduce oxygen functional group and improve the electrical and mechanical properties of materials. The Krf excimer laser has energy of 700mj, pulse width of 20ns, wavelength of 248nm, and working distance to quartz tube of 30cm. There is a noticeable change in the colour of graphene oxide solution from yellow-brown to black, which is clear evidence of reduction [24].

The change in graphene oxide solution after pulsed laser irradiation was evaluated by Raman spectroscopy using 632nm laser. Raman spectra measured a range of 1000 to1800 cm^{-1}. In Figure 3-11 two peaks appear for GO film which are D in 1336cm^{-1} related to structure disorder and G in 1586cm^{-1} related to sp^2 bonded carbon. The peaks shifted on rGO film at a lower energy level, so D appears at 1327cm^{-1}, and G at 1584cm^{-1}. Calculating the intensity ratio of D and G band can provide information regarding defects and disorders [24].

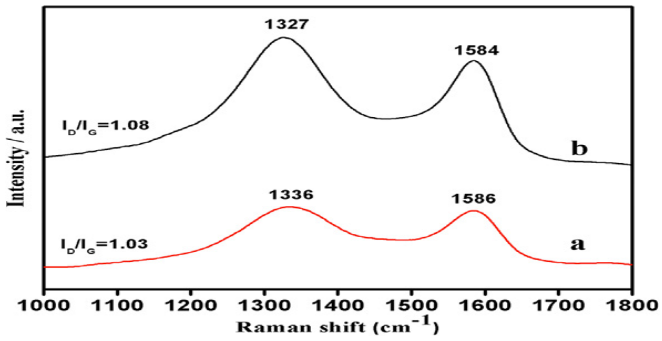

Figure 3-11: Raman Spectra (a) GO, (b) rGO [24]

3.4.4 Reduced graphene oxide with ethanol and thermal annealing

In recent study, ethanol can facilitate the reduction of graphene oxide multilayer sheet during thermal annealing [25]. Although the mechanism of reduction is still under investigation, ethanol can reduce (C=O) in graphene sheet and restoring of the carbon conjugation structure. For example, the efficiency of reduced graphene oxide was measured with alcohol mixed with graphene oxide studies by FTIR during annealing at different temperatures from 60°C to 200°C. Figure 3-12 shows the difference in FTIR absorbance between methanol and ethanol mixed with graphene oxide [25].

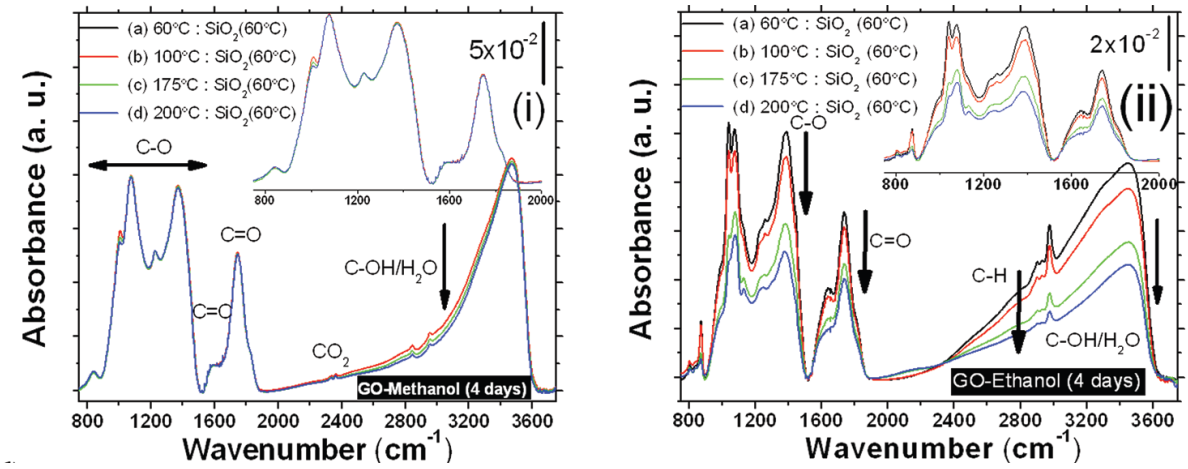

Figure 3-12: (i) FTIR spectra of GO intercalate with methanol; (ii) GO mixed with ethanol [25]

Chapter 4: Research Objectives, Reduced Graphene Oxide Methods, and Characterization Tools

4.1 Introduction

The main goal of this research is to study the optimal conditions for fabrication of reduced graphene oxide film through spin-cast and vacuum filtration techniques, respectively. This investigation begins by fabricating of graphene oxide films on the silicon wafer and silica glass substrates by means of spin-cast method using diluted and undiluted graphene oxide solution with different concentrations. The effect of baking temperature and baking time on graphene oxide film properties was studied in terms of defect and surface morphology. The photo- reduction approach was also employed to reduced graphene oxide film using deep UV light.

4.2 Experiments and methodology

Graphene oxide solutions were purchased from Graphene Supermarket Inc. at different concentrations of 500mg/l (LC) and a high concentration of 6.2g/l (HC). The LC solution consisted of a single layer of graphene oxide dispersed in 175ml water. Carbon atoms comprised 79% of the entire solution while oxygen atoms comprised 20%. The flake size

was approximately 0.3-0.7μm and 0.5-5μm in LC and HC graphene oxide solutions respectively, with thickness of one atomic layer.

Atomic force microscopy (AFM-Dimension 3100 scanning probe microscope) was employed to characterize the surface morphology of the fabricated graphene oxide films. Dual-wavelength micro-Raman spectrometer with excitation wavelength of 632.8nm from Renishaw Rama spectrometer was used to study the effects of low temperature heat treatment and deep UV light exposure treatment on the structural properties of graphene oxide films. The surface morphology of deposited reduced graphene oxide films was studied by means of field emission scanning electron microscope (SEM). Fourier Transform infrared (FTIR) spectrometer (FT-IR 8400s Shimadzu Corp.) was used to study the molecular vibration spectroscopy of graphene oxide films before and after reduction procedure. The UV-VIS spectrometer (UV-2501PC from Shimadzu Corp.) with resolution of 0.1nm and accuracy of 3nm was utilized to compare the electronic absorption of graphene oxide and reduced graphene oxide films.

4.3 Methods of reducing graphene oxide

Several methods are used to remove functional group that attaches to graphene oxide sheet and destroy its electrical properties. In this research, I attempt to investigate the effect of multistep reduction, since using only one method is insufficient to completely remove D band from Raman spectra. First, graphene oxide films annealed at low temperature; next, graphene oxide is mixed to form a solution with ethanol; and finally photo reduction is subsequently employed.

Chapter 5: Reduced Graphene Oxide Film by means of Annealing at Low Temperature

5.1 Introduction

Heating GO film at different temperatures and times can significantly affect the electronic properties of the deposited film. The conductivity of GO film is reduced by the existence of carbon and oxygen functional groups at the edge and in plane of the GO sheets, respectively. In the GO sheet carboxyl (COOH),carbonyl (C=O) and ester (COO) groups are presented at the edge sheet structure [5]. In the oxygen functional group, epoxy (C-O-C) and hydroxyl (C-O) groups are observed as in plane chemical bonds [5]. Annealing GO film at high temperature can lead to removal of the carbon and oxygen functional groups and improve the conductivity of GO sheet. However, this process could potentially introduce more vacancy and defects. The mechanism of reducing the oxygen and carbon functional groups from GO sheet and restoring conjugation structure is not well understood. Thus, healing defects and rearranging of carbon atoms after the reduction process is still under investigation [5].

5.2 Experiments

The experimental procedure of reduce functional groups followed several steps. First, quartz substrate was washed by deionized water, acetone, and isopropanol, followed by drying by nitrogen gas. In the second step, substrate was mounted on the spinner and the GO film was grown using a spinning speed of 3000 rpm for 30 seconds. In the last step, the deposited GO films were baked at different temperatures in the range of 60^{o}C to 90^{o}C and at baking times in the range of 10min to 40min. Raman spectroscopy was carried out to study the effects of baking temperature and baking time on the structural defects of rGO films, as shown in Figure 5-1. The rGO film surface profile and surface roughness were studied using AFM and are compared in Figure 5-2.

5.3 Characterization

5.3.1 Raman spectroscopy characterization

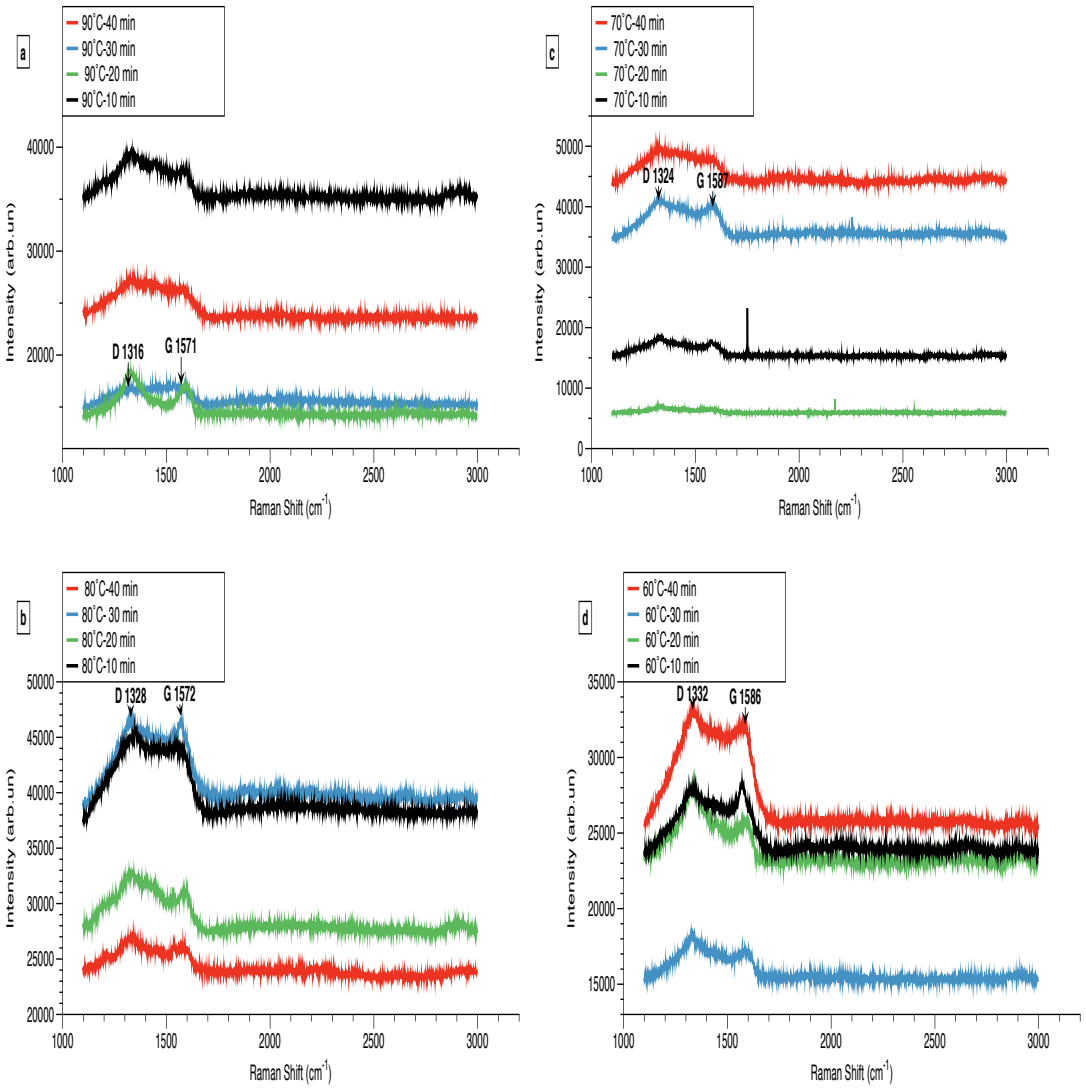

Figure 5-1: Recorded Raman spectrum of rGO films at different baking temperatures and baking times

Table 5-1: Calculations of ID/IG of rGO films at different baking temperatures and baking times

Time	90°C ID/IG	80°C ID/IG	70°C ID/IG	60°C ID/IG
40 min	1.02	1.03	1.03	1.03
30 min	0.98	1.00	1.02	1.06
20 min	1.06	1.05	1.07	1.08
10 min	1.04	1.05	1.08	1.09

Generally, reduced graphene oxide can be evaluated from calculating ID/IG. Any slight modification in reduction procedure can be observed by calculating ID/IG. In fact, ID/IG is widely used to measure the distance between defects in graphene oxide samples. For example, using 532nm laser excitation gives ID/IG of 1 of graphene oxide film. However, this ratio increases to a maximum of 3 during reduction process, which indicates an increased distance between defects, followed by a decrease [26]. Moreover, the essentially feature of graphene oxide Raman spectra are D band ranging from 1330-1340cm^{-1}, and G band ranging from 1580-1600cm^{-1} [26]. Raman shift for G band from higher frequency of 1590cm^{-1} to lower frequency of 1571cm^{-1}, indicates that graphene oxide structure is almost modified to graphite structure [14].

From Raman spectrums in Figure 5-1 and intensity ratio ID/IG in Table 5-1, it can be concluded that annealing samples for 30min gives a lower ID/IG, in particularly temperatures of 90°C, 80°C, and 70°C. Increasing of backing time to 40min causes an increased ID/IG ratio. However, in terms of annealing samples at temperature of 60°C, 40 min annealing gives a lower intensity ratio of 1.03 compared to other samples. Since ID/IG is a correlated by defect and disorder in the materials, lower ID/IG indicates lower defect and increased

crystal structure of materials. By selecting lower ID/IG samples in Table 5-1, and determing Raman shift of D, and G band, it is possible to determined which sample has a structure that is close to graphite structure (Table 5-2).

Table 5-2: D and G band Raman shift for lower ID/IG ratio samples

Temperature and baking time	D band position in X-axis	G band position in X-axis	ID/IG in Y-axis
90^{o}C – 30 min	1316 cm^{-1}	1571 cm^{-1}	0.98
80^{o}C – 30 min	1328 cm^{-1}	1572 cm^{-1}	1.00
70^{o}C – 30 min	1324 cm^{-1}	1587 cm^{-1}	1.02
60^{o}C – 40 min	1332 cm^{-1}	1586 cm^{-1}	1.03

From Table 5-2 , it can be concluded that annealing sample at temperatures of 90^{o}C and 80^{o}C shows lower defect ratio with structures that are close to graphite. G band shifted to a lower frequency level from 1586cm^{-1} to 1571cm^{-1}, at high temperatures of 90^{o}C and 80^{o}C.

5.3.2 AFM characterization

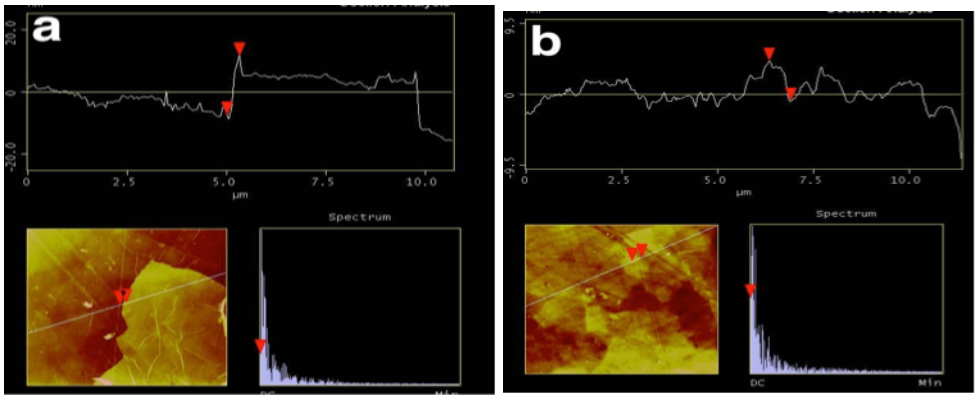

Figure 5-2: AFM image of GO film annealed at (a) 90°C for 30min; and (b) at 60°C for 10min

The AFM image of samples annealed at 90°C for 30min and 60°C for 10min reveal a trade-off. While increasing baking temperature to 90°C and time to 30min can significantly remove functional groups and decrease the distance between defects; on the other hand, it also causes increases in film thickness and roughness. It was found that the GO flake size and the flake surface roughness were reduced from 19.7nm and 1.4-8nm to 5nm and 0.7-2.5nm, respectively, by reducing the baking temperature from 90°C to 60°C, as can be seen from Figure 5-2. Therefore, it can be concluded that the ratio of ID/IG and surface roughness of the GO film were increased by annealing the GO films at a low temperature for more than 30min.

5.4 Conclusion

It has been found in many published papers that annealing graphene oxide film at high temperature causes removal of oxygen functional groups as well as carbon atoms [6]. This result is supported by Raman spectroscopy spectrum, which revealed the absence of 2D band. The absence of 2D band after annealing graphene oxide film at high temperature indicate damage in graphene oxide sheet [6]. This experiment studied the effect of annealing at low temperature on graphene oxide film properties. In fact, Raman spectrum indicates slight reduction of oxygen functional groups, as observed from D,G band shift and in the intensity of ID/IG. However, D band, which is related to defects, still appeared on all of the samples. Moreover, atomic force microscopy images show that annealing sample for 90^{o}C, increases film thickness and roughness.

Chapter 6: Reduced Graphene Oxide by means of Dilution with Ethanol

6.1 Introduction

There are in plane and out plane carbon and oxygen functional groups such as epoxide, hydroxyls, and carbonyl which are difficult to reduce even at high annealing temperatures. Mixing the GO solution with ethanol could be an effective approach to reducing the oxygen functional groups and replacing with carbon functional groups. Modifying graphene oxide solution before fabricating the film could reduce the vacancy that is generated in the film as a result of removing oxygen groups. Diluting graphene oxide solution with ethanol exhibit a environment friendly method in reduced graphene oxide film.

6.2 Experiment

In order to compare the effects of diluted LC and HC GO solutions with undiluted solutions , three graphene oxide solutions were prepared: graphene oxide dispersed in water, and 1 ml GO solution diluted in 5ml ethanol, and 1ml GO solution diluted in 10ml ethanol. The structural properties and film surface morphologies of deposited diluted LC and HC GO films were studied by using Raman, XPS spectroscopy and AFM. In addition to characterizing the film, graphene oxide solution was characterized by FTIR, and UV-VIS.

6.3 Characterization

6.3.1 UV-VIS spectroscopy characterization

The UV-VIS spectroscopy was utilized to study the effects of reduction procedure on absorption of the carbonyl groups. The absorbance of LC and HC GO before diluting with ethanol was significantly larger than before diluting, which was impossible to identify, as shown in Figures 6-1(a) and 6-1(b). However, after diluting LC GO solutions with 5ml ethanol, two absorption peaks were recorded at wavelengths of 230nm ($\pi \rightarrow \pi^*$) and 290nm($n \rightarrow \pi^*$) which are attributed to C=C and C=O bonds, respectively [18]. Increasing ethanol concentration from 5ml to 10ml in 1ml GO solution reduced the C=O absorbance, which could be attributed to the oxygen components reduction as is evident in Figure 6-1 (a)(b) [18].

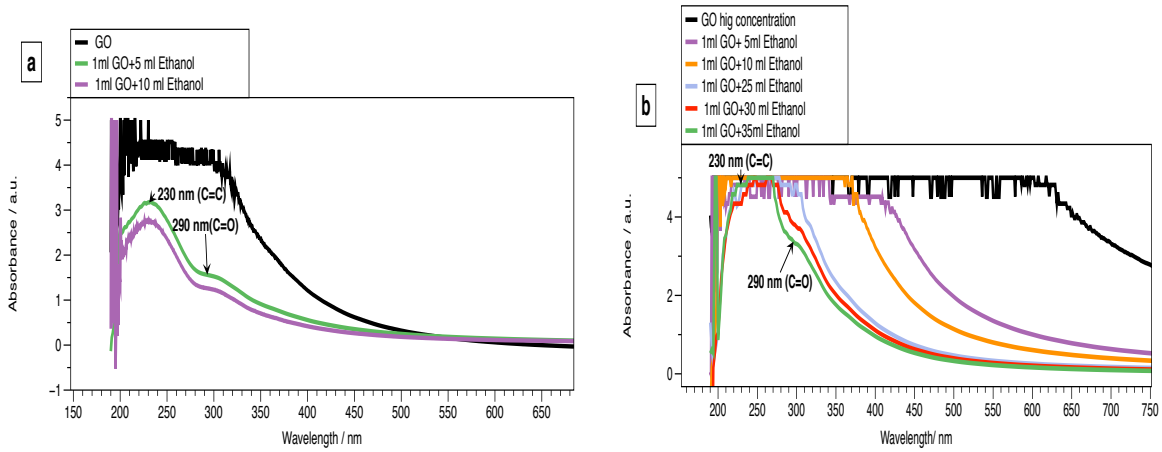

Figure 6-1: The UV-VIS spectrum of (a) LC GO; and (b) HC GO solution before and after dilution with different ethanol concentrations

By using HC GO solution, 10ml ethanol was found to be insufficient to identify epoxy and carbonyl absorption. It was found that these absorption peaks could be recorded by UV-VIS spectrometer in diluting the HC GO solutions with 35ml ethanol, as illustrated in Figure 6-1(b).

6.3.2 FTIR spectroscopy characterization

Additional molecular analysis of diluted and undiluted LC and HC GO solutions were studied by employing FTIR Spectroscopy. Figure 6-2 shows the FTIR spectrum of LC and HC GO solutions before and after diluting with different concentrations of ethanol.

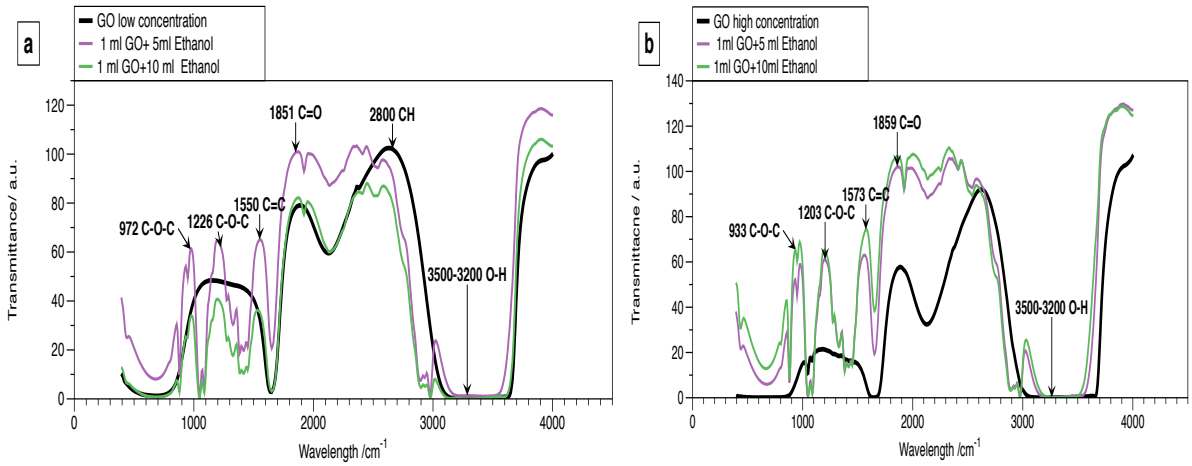

Figure 6-2: Recorded FTIR spectrum of (a) LC; and (b) HC GO solution before and after diluting with 5ml and 10ml ethanol

As evident in Figure 6-2, the transmittance of both LC and HC GO solutions was increased by removal of oxygen functional groups. It was found that by diluting the LC GO solutions with 5ml ethanol, the transmittance of oxygen functional groups at wavenumbers of 972cm^{-1} (C-O-C) [27], 1550cm^{-1}(C=C) [27], and 1851cm^{-1} (C=O) [27] as shown in Figure 6-2(a). Increasing the ethanol concentration to 10ml increases the reduction process and improves the transmittance of the GO solutions.

Diluting HC GO solution with 5ml and 10ml ethanol exhibited a similar trend. Both diluted HC GO solutions showed an increase in transmittance with a similar level of reduction compared to the level of reduction in undiluted HC GO solution Figure 6-2(b). The transmittance of oxygen functional group at wavenumbers of 933cm^{-1} (C-O-C) [27], 1573cm^{-1} (C=C), and 1859cm^{-1} (C=O) [27] increased significantly compared with undiluted .

6.3.3 Raman spectroscopy characterization

The undiluted and diluted LC GO films were fabricated using silicon substrate and spin cast method at spinning speed of 3000rpm. The deposited films were baked at 90^{o}C for 30min. Figure 6-3 shows the recorded Raman spectrum of LC GO films before and after diluting with 10ml ethanol.

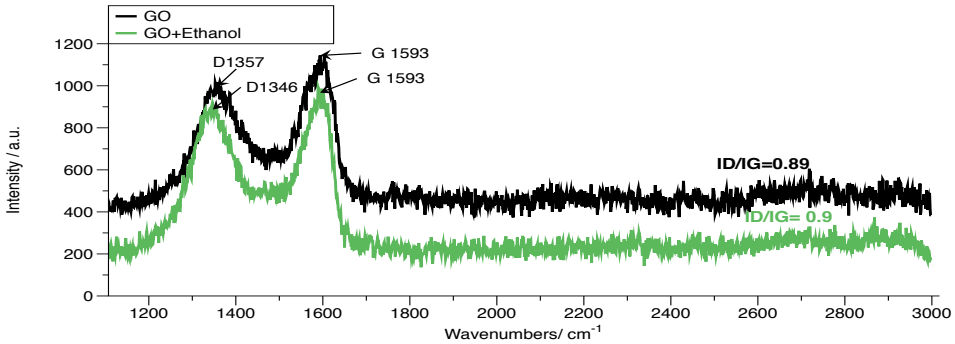

Figure 6-3: Raman spectrum of LC GO: Black represents undiluted GO film, and green represents diluted GO film made from mixture (1ml GO+10ml ethanol)

As can be seen from Figure 6-3, by diluting the LC GO solutions with 10ml ethanol, the molecular vibration band at wavenumber of 1357cm^{-1} (D-band) shifted towards smaller wavenumbers by 9cm^{-1}, which could be due to the removal of oxygen functional groups. However, there were no changes in the molecular vibration of G band as wavenumber of 1593cm^{-1}. The ID/IG ratio for both diluted and undiluted LC GO films were calculated as 0.9, which indicates that there were no structural defects in both fabricated LC GO films.

6.3.4 AFM characterization

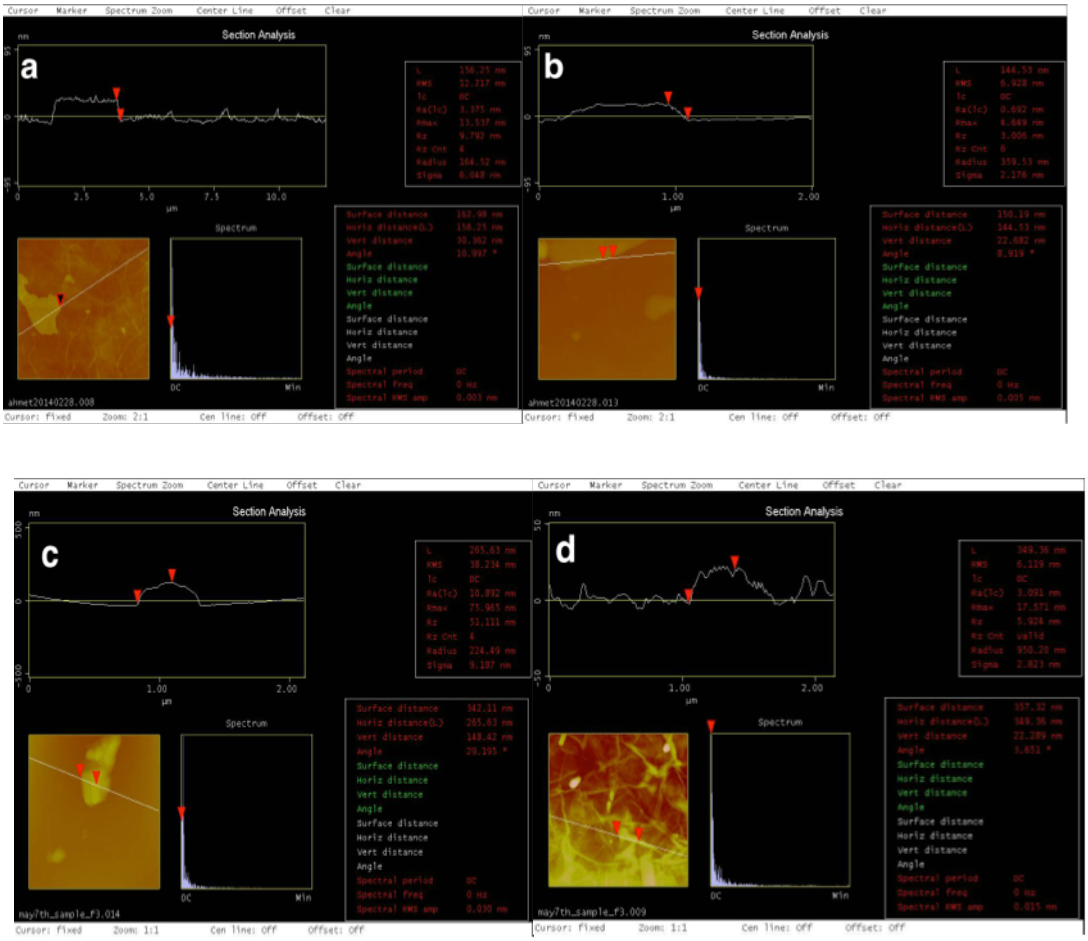

Figure 6-4: AFM image of LC GO (a) Undiluted GO film; (b) Diluted GO+ 10ml ethanol film and HC GO; (c) Undiluted GO film; (d) Diluted 1ml GO+ 35ml ethanol

A series of thin films were fabricated from undiluted LC and HC GO solutions and diluted GO solutions with 10ml ethanol and 35ml ethanol using spin casting method at a spinning speed of 3000rpm, baking temperature of 90^{o}C, and baking time of 30min. The surface morphology of fabricated films were studied using AFM.

Figure 6-4 (a-b) shows the AFM images of undiluted and diluted LC GO films. As can be seen from this figure, the thickness of GO flakes was reduced from 30.36nm to 22.68nm by diluting the LC GO solutions with 10ml ethanol. The surface roughness of the GO flakes was reduced from 3.37nm to 0.69nm as a result of diluting the LC GO solutions with 10ml ethanol and reducing the oxygen functional groups.

The AFM images from high concentration graphene oxide films which were undiluted and diluted with 35ml ethanol in Figure 6-4 (c,d) shows results similar to low concentration graphene oxide. Thickness of graphene oxide flakes was reduced from 148nm to 22nm by diluting the HC GO with 35ml ethanol. In addition to film thickness, surface roughness was reduced from 10nm to 3nm.

6.3.5 XPS spectroscopy characterization

Chemical analyses of fabricated GO thin films from undiluted and diluted (10ml ethanol:1ml GO solution) of the LC and HC GO solutions were carried out using XPS. In this study the thin films were fabricated on silicon substrate using the spin cast method at different spinning speeds of 3000rpm and 6000rpm. The other fabrication parameters were fixed at baking temperature of 90^{o}C and baking time of 30min. For each sample, the carbon/oxygen atomic ratio, the FWHM of carbon functional groups and oxygen atoms, and the binding energy variations of each chemical bond were analyzed using recorded XPS spectrum.

Figure 6-5 shows the recorded XPS spectrum of fabricated LC GO thin films at spinning speed of 3000rpm and 6000rpm.

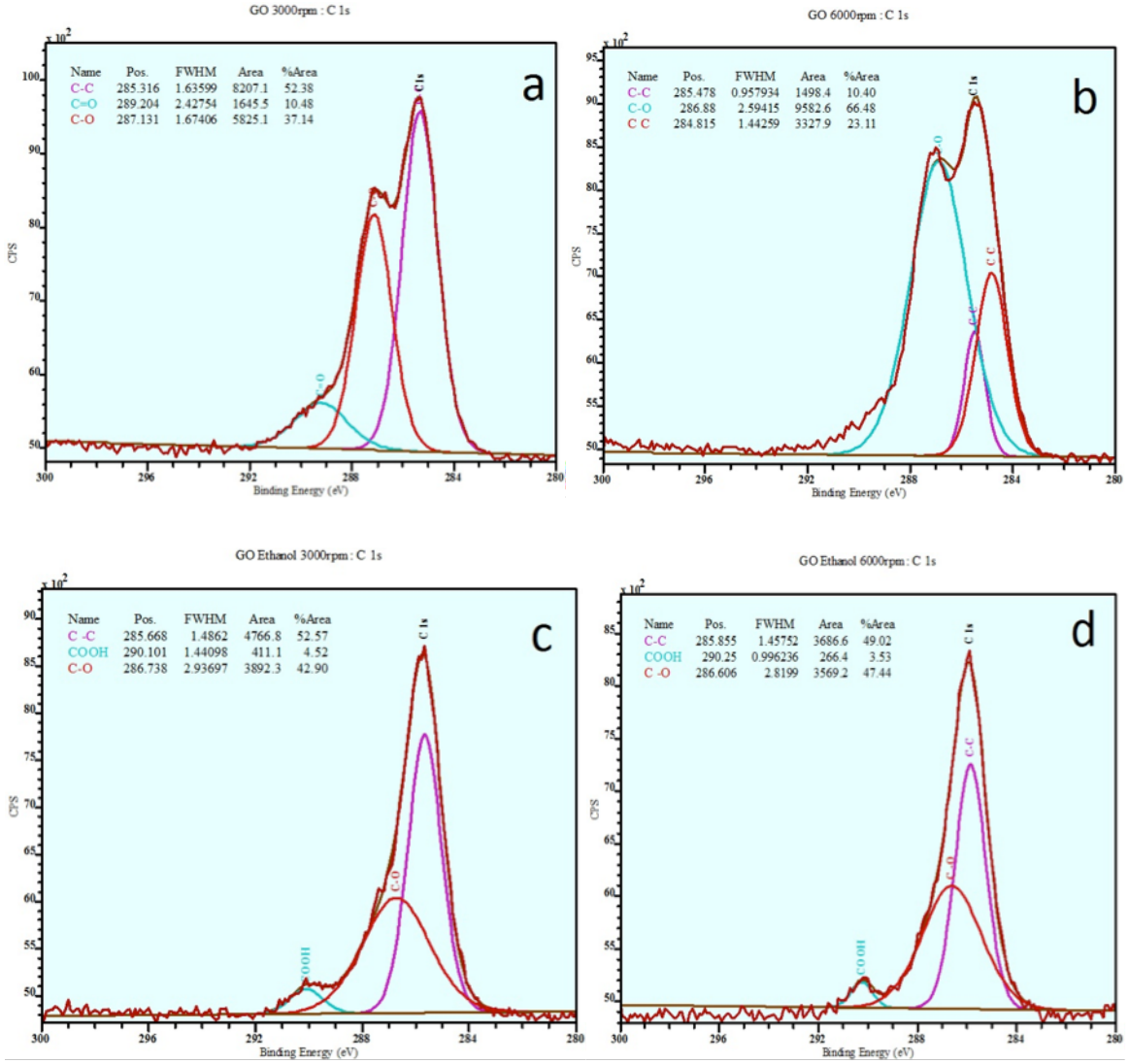

Figure 6-5: Recorded XPS spectrum of LC GO films fabricated at spinning speeds of a) 3000rpm; b) 6000rpm; and diluted GO films (1ml GO+10ml ethanol) at spinning speed of c) 3000rpm; d) 6000rpm

X-ray photoelectron spectroscopy (XPS) was also performed to analyze samples before and after dilution with ethanol. In addition, the effect of rising the spinner speed from 3000rpm to 6000rpm was evaluated in chemical bonding. The XPS spectra for C1s from LC GO before and after dilution with 10ml ethanol at different spinner speeds are shown in Figure 6-5. The XPS curves were fitted by three peaks in GO undiluted film in correspondence to the following binding energy ~284ev (C-C), ~285ev (C C), and ~287ev (C-O) [28]. However, LC (1ml GO+10ml ethanol) films showed a peak binding energy of ~290ev (COOH) [28]. It was found that the presence of Ethanol can significantly decrease C-O, and C=O ratio compared with untreated GO samples [25]. By comparing samples (a) and (c) in Figure 6-5, it is clear that both samples have similar film thicknesses; however, there are differences in chemical composition. Sample (c), which was treated with Ethanol, shows removal of C=O and formation of COOH, which is easily removed during thermal reduction [25]. Similarly, by comparing thinner films in samples (b) and (d), there is reduction of C-O and formation of COOH, which is easily dissociated according to the molecular dynamic simulation [25].

6.4 Conclusion

It has been found experimentally that alcohol can reduce oxygen atoms in graphene oxide solution. Ethanol can remove oxygen atoms and restore hexagonal structure with a lower amount of defects [25]. In this research, LC/HC graphene oxide solution was diluted with different percentages of ethanol and characterized with as film or solution by a variety of instruments. UV- VIS in Figure 6-1 shows a decrease in carbonyl absorption peak after an increase in ethanol concentration to 10ml. In addition to UV-VIS, FTIR transmittance from LC/HC GO solution increased after dilution with 5/10ml ethanol compared with untreated GO solution. Raman spectroscopy, which is a sensitive technique in measuring reduction, shows a reduction in FWHM for D band after dilution with 10ml ethanol. In terms of graphene oxide flake thickness and roughness, film made from mixture of graphene oxide and ethanol shows reduced film thickness and roughness compared with undiluted film. Finally, XPS atomic ratio shows complete removal or decrease of C=O, and formation of COOH instead which has a lower energy bond [25].

Chapter 7: Reduced Graphene Oxide Films with UV-Light Exposure

7.1 Introduction

Recently, photo reduction has reported an environmentally friendly approach to fabricating reduced graphene oxide film. Although chemical reduction can remove oxygen functional group effectively, it can cause impurities that affect graphene oxide film properties. Photo reduction can break the bond between graphene sheet and oxygen functional group with less impurities [8].

7.2 Experiment

Fabricated GO thin films from diluted and undiluted HC and LC GO solutions at spinning speed of 3000 rpm and baking temperature and time of 90^{o}C and 30min, respectively, were exposed by deep UV light at wavelengths of 190-400nm for different exposure times ranging from 2hrs to 8hrs.

Structural characterization and surface morphology of irradiated GO films were studied using Raman spectroscopy and SEM, respectively. Raman spectroscopy was carried out after each exposure. However, the SEM of exposed samples were carried out before and after final exposure to UV-light.

7.3 Characterization

7.3.1 Raman spectroscopy

Figure 7-1 shows the effects of different exposure times on the molecular structure of diluted and undiluted LC and HC GO films before and after UV treatment.

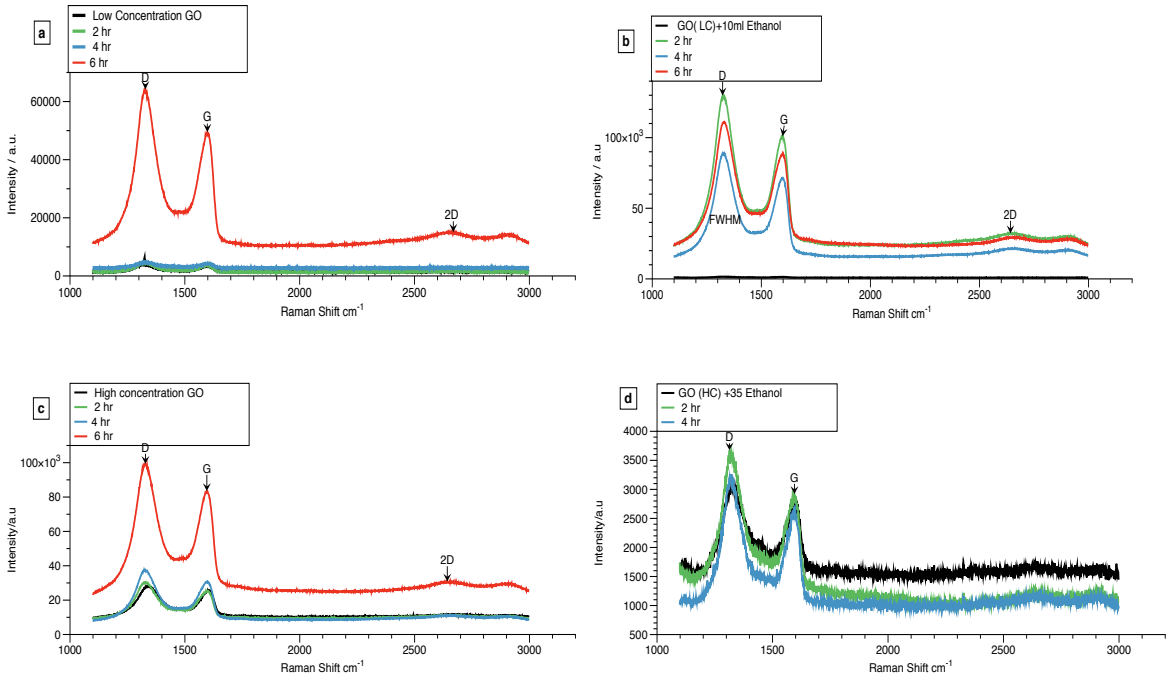

Figure 7-1: Raman spectrums form HC/LC GO undiluted and diluted with ethanol films. (a) LC GO film; (b) LC(1ml GO+35ml ethanol) film; (c) HC GO; (d) HC (1ml GO + 35ml ethanol) film

Table 7-1: Record of D and G bands positions, Intensity of ID/IG ratio and I2D/IG ratio, and D band FWHM of undiluted and diluted LC and HC GO films before and after deep UV treatment.

(a) GO 500mg/l film						
Exposure time	D cm^{-1}	G cm^{-1}	ID/IG cm^{-1}	FWHM (D)	2D cm^{-1}	I2D/IG
0	1335	1601	1.1	180		0.47
2hr	1325	1599	1.2	141		0.44
4hr	1324	1605	1.1	150		0.6
6hr	1328	1593	1.3	188	2655	0.3
(b) GO 500mg/l +10ml Ethanol						
Exposure time	D cm^{-1}	G cm^{-1}	ID/IG	FWHM (D)	2D cm^{-1}	I2D/IG
0	1337	1596	1.1	221		0.6
2hr	1325	1593	1.2	132	2650	0.3
4hr	1323	1594	1.2	133	2655	0.3
6hr	1323	1599	1.2	180	2651	0.3
(c) GO 6.2 g/l						
Exposure time	D cm^{-1}	G cm^{-1}	ID/IG	FWHM (D)	2D cm^{-1}	I2D/IG
0	1339	1605	1.1	195		0.4
2hr	1328	1593	1.2	172		0.4
4hr	1324	1593	2.3	149		0.3
6hr	1323	1593	1.1	156	2646	0.3
(d) GO 6.2 g/l + 35 Ethanol						
Exposure time	D cm^{-1}	G cm^{-1}	ID/IG	FWHM (D)	2D cm^{-1}	I2D/IG
0	1335	1604	1.1	250		0.6
2hr	1328	1589	1.1	265	2636	0.6
4hr	1323	1590	1.2	157	2644	0.4

The position of D and G bands and FWHM in the Raman spectrum are highly sensitive to the existence of the carbon and oxygen functional groups in the GO films [29]. The presence of disorder and defects in the GO films can be investigated by analyzing the D band intensity and by broadening of the G and D bands [29].

Figure 7-1 (a) shows the Raman spectrum of LC GO films at different exposure time. As can be seen from this figure, the 2D band was recorded at wavenumber of 2655cm^{-1} after 6hrs UV treatment, which could be attributed to the removal of oxygen component and graphene formation [7]. It was also found that the G band position shifted from 1601cm^{-1} by 8cm^{-1} toward a smaller wavenumber. The effects of longer exposure time were observed to increase the GO film's disorders and defects by increasing D band intensity and FWHM from 180cm^{-1} to 188cm^{-1}. Figure 7-1(b) shows the Raman spectrum of diluted LC GO films. As can be seen in Table 7-1(b), the 2D band was recorded at wavenumber of 2650cm^{-1} followed by reducing the FWHM value of the D band by 132cm^{-1} after 2hrs UV treatment. There were no significant changes in the position of D and G band after longer exposure time as is clear from Table 7-1(b); however, the FWHM of D band was increased by 180cm^{-1} as a results of increasing the exposure time to 6hrs.

Figure 7-1(c,d) shows the Raman spectrum of undiluted and diluted HC GO films. As can be seen from Figure 7-1(c), the 2D band was recorded at wavenumber of 2646cm^{-1} after 6hrs UV light treatment followed by significant increases in D band intensity. Although the ratio was increased by increasing the exposure time from 0 to 6hrs and reached its maximum at 2.3 after 4hrs exposure, by increasing exposure time to 6hrs the ID/IG ratio was calculated as

1.1 which could be attributed to the structural modification defect reduction. Figure 7-1(d) shows that when HC GO was diluted with ethanol, 2D band formed after 2hrs UV exposure with ID/IG ratio of 1.1 similar to ID/IG before exposure to UV. Further increase to 4hrs can cause decrease in D band FWHM from 250cm^{-1} to 157cm^{-1}. Generally. the I2D/IG ratio is an indication of the number of layers in the graphene thin films [12]. As evident in Table 7-1, the I2D/IG was calculated as 0.3 which is attributed to multilayer graphene films.

7.3.2 SEM characterization

The SEM was employed to study the effects of UV treatment on LC and HC GO films. Figure 7-2 shows SEM images of LC GO films before and after deep UV treatment.

As can be seen from Figure 7-2(a), the GO flakes are aggregated GO before UV treatment in the LC GO film. Although the aggregated flakes are large, they only cover some part of the LC GO films. It was found that after 6hrs UV treatment, the GO flakes covered the entire film surface with smaller particle agglomeration and finer crystalline structure, as shown in Figure 7-2(b). Figures 7-2(c) and 7-2(d) compare the effects of UV treatment on the surface morphology of diluted LC GO films. As can be seen from Figure 7-2(c), the number of aggregated GO flakes (bright objects) were significantly reduced followed by reduction of GO flake dimensions compared to undiluted LC GO films (Figure 7-2(a)). Figure 7-2(d) shows the LC GO flake after 6hrs UV exposure. As can be seen from this figure, the ethanol residue is completely removed after UV exposure and the GO flake sizes are reduced. While undiluted GO flakes were easily observed from range of 10μm, diluted GO flakes were observed in range of 1μm due to small dimension and high level of dispersion .

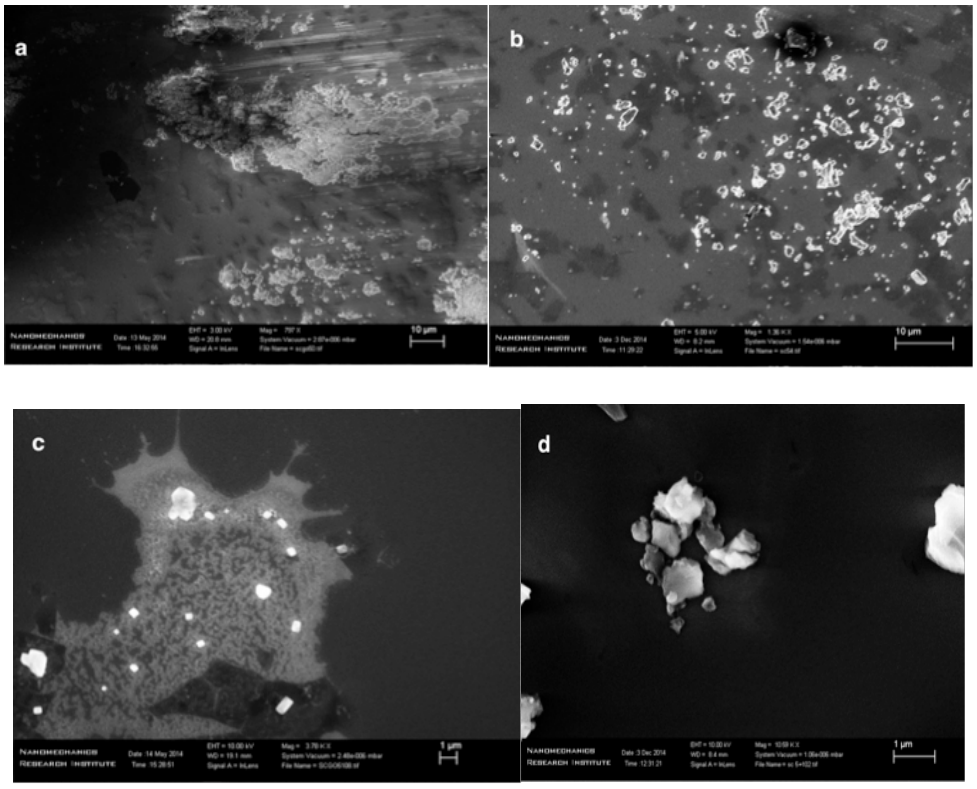

Figure 7-2: SEM images LC undiluted GO films (a) before and (b) after UV treatment; and diluted GO films with 10ml ethanol (c) before and (d) after UV treatment

The effects of UV treatment on the HC GO films surface morphology are compared in Figures 7-3(a-d) for both undiluted and diluted GO films. Figure 7-3 (a-b) compares the effects of UV irritation on the undiluted HC GO films. As is clear that the GO flakes were multilayer and their sizes were larger in comparison to the LC GO films. It was found that by using the deep UV treatment, the large GO flakes broken into small GO flakes; however, they were aggregated to each other, as evident in Figure 7-3(b). The HC GO solutions were diluted with 35ml ethanol. The effects of 6hrs UV treatment on the surface morphology of

the HC GO films are compared in Figure 7-3(c-d). After 6hrs exposure, small flakes and less aggregation were found in comparison with the UV exposed LC GO films.

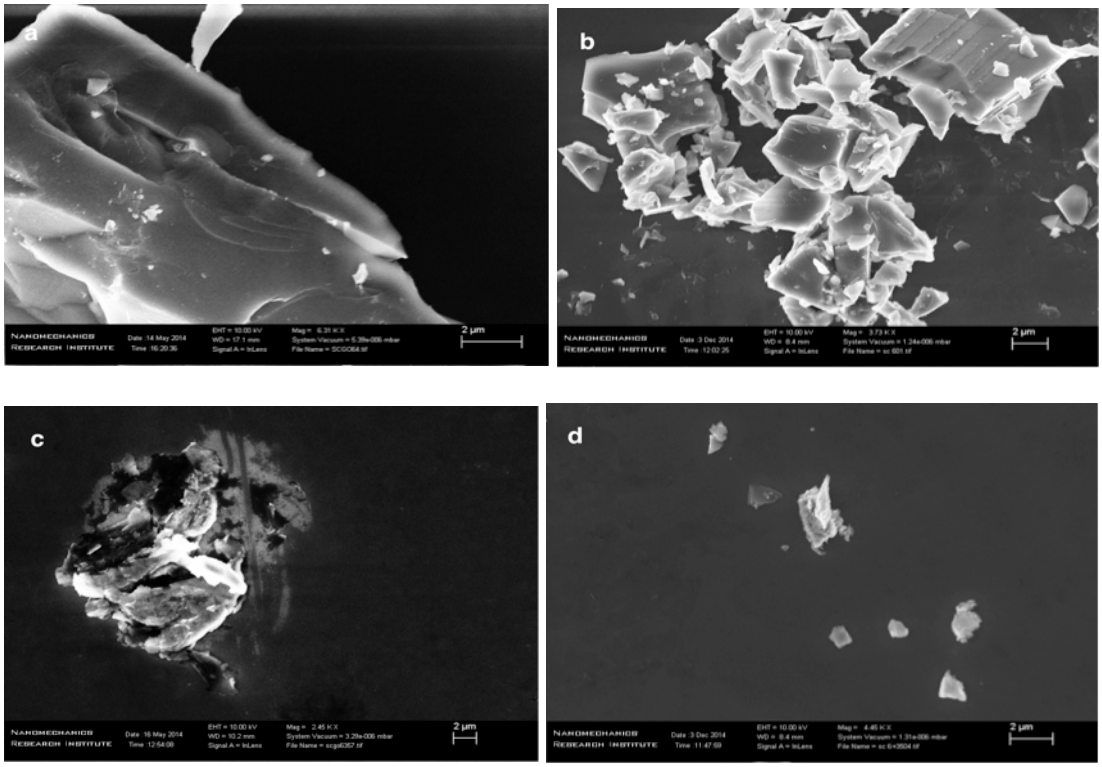

Figure 7-3:SEM images of HC undiluted GO films (a)before and (b) after UV treatment and diluted with 35ml ethanol; and (c) before (d) after UV treatment

7.4 Conclusion

Although there are a several methods in fabricating reduced graphene oxide, photo reduction approach shows advantages over other technique as a clean , fast method. This experiment utilized three steps to fabricate reduced graphene oxide film after diluted with ethanol and annealed at low temperature. Rama spectroscopy, which is a sensitive technique to evaluate

the efficiency of reduction, was used after each 2hrs UV treatment. In general, the entire graphene oxide films that were made from LC/HC GO diluted and undiluted show successful reduction of oxygen functional group and formation of graphene band in ~2700cm^{-1}. However, undiluted HC/LC GO sample showed higher D band intensity compared with diluted HC/LC GO films with ethanol. This result could be attributed to the presence of ethanol which has a capability to heal defects [25]. Furthermore, films that were prepared from a mixture of GO and ethanol consumed less energy in the reduction process. Diluted HC/LC GO films showed formation of graphene after 2hrs exposure to UV-light, and undiluted sample needed more than 6hrs UV treatment to narrow the D band and increase the intensity of the 2D band.

In terms of surface morphology, SEM images of LC GO undiluted and diluted showed less aggregation of GO flakes after 6hrs UV treatment. However, the dimensional of GO flakes was smaller in the case of the diluted sample, with the image in the range of 1μm, compared to 10μm in undiluted sample. However, in terms of HC GO films, undiluted GO film showed a rough surface and an aggregation of GO flakes even after 6hrs UV exposure. Image of diluted HC GO with 35 ethanol image showed a uniform film with asmaller GO layer.

Chapter 8: Reduced Graphene Oxide Paper through UV Light Treatment

8.1 Introduction

Fabrication of GO film with engineered thicknesses (number of layers) ranging from nanometer to micrometer has been an interesting topic of research since 2004.

Deposition methods such as drop casting, dip coating, and rapid freezing can affect the electrical, mechanical, and optical properties of GO films. Recently, uniform GO membrane ranging from single layer to several layers were fabricated using vacuum filtration [30] and cellulous ester membrane to filter graphene oxide solution. The membrane had a pore size of 25nm which allowed the solvent to pass through the pores and collect GO flakes [31]. Filtration rate decreased noticeably by increasing the filtration time due to the accumulation of the GO layers on the membrane surface. The thickness of the filtered film can be controlled by changing filtration volume and GO concentration [31]. The GO film can be transferred to the substrate by etching the membrane in a proper solution, as shown schematically in Figure 8-1, followed by annealing at a high temperature such as 550^{o}C to remove the etchant residual.

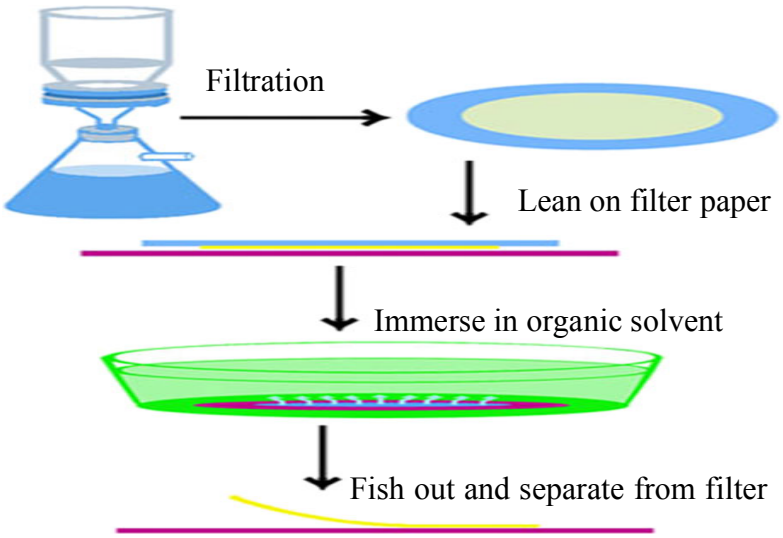

Figure 8-1: Schematic diagram of graphene membrane fabricated using vacuum filtration method [31]

8.2 Experimental

In this experimental a filter from Whatman Anodisc 25 was used with a pore size of 0.02µm and 25mm diameter. Under vacuum condition, graphene oxide solution passed through the filter. The filter worked to collect graphene oxide flakes and remove the solvent. Next, the film was baked at 50^{o}C for 6hrs, followed by graphene oxide membrane being dissociated in HCL. The floating membrane was transferred to Si substrate and left to dry.

8.3 Characterization

8.3.1 Raman spectroscopy characterization

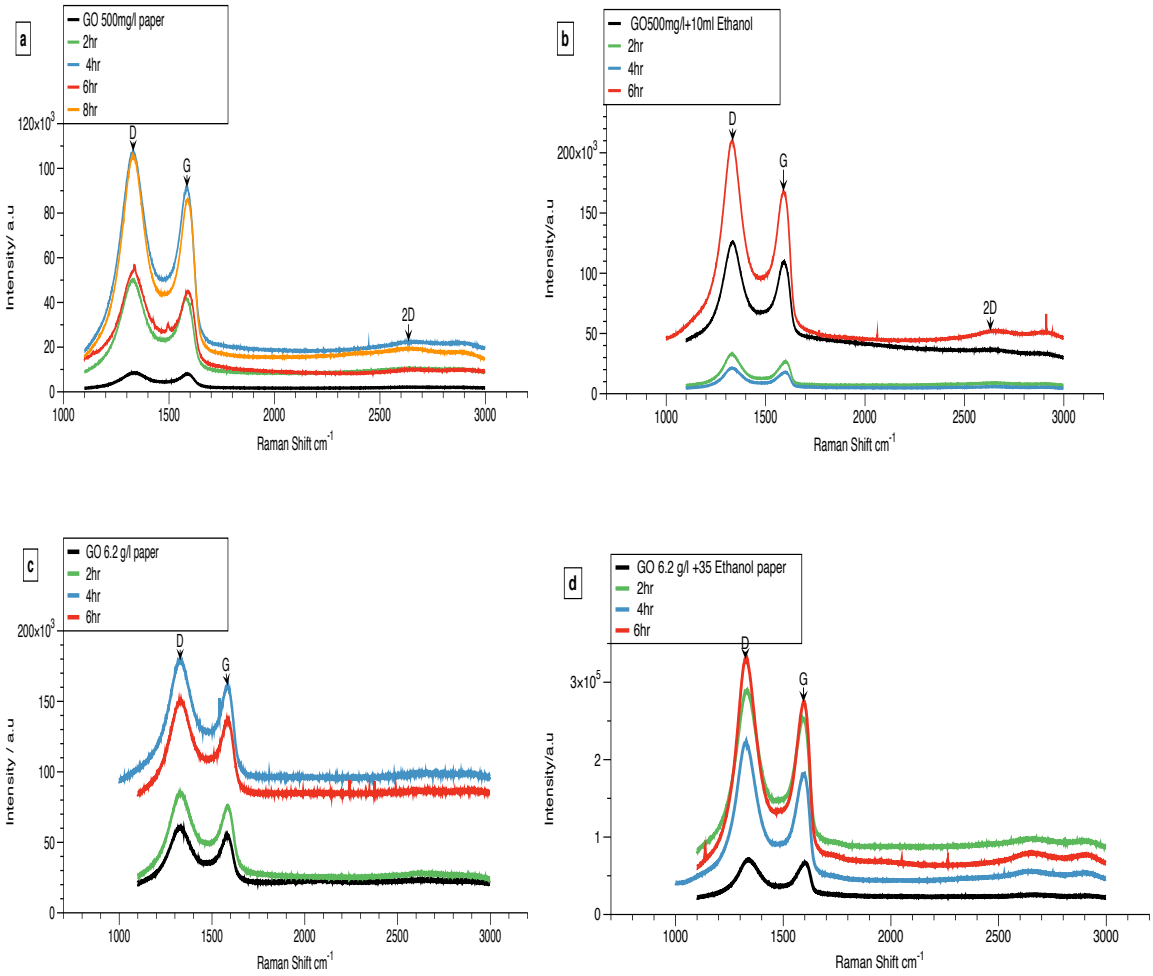

Figure 8-2: Recorded Raman spectrum of (a) Undiluted LC; (b) Diluted LC; (c) Undiluted HC; and (d) Diluted HC GO paper before and after different deep UV exposure time.

Table 8-1: Recorded D band and G band position, intensity, FWHM, ID/IG, and I2D/IG of undiluted and diluted LC and HC GO. The GO films were fabricated by means of vacuum filtration method

Go 500mg/l paper						
Exposure time	D	G	ID/IG	FWHM (D)	2D	I2D/IG
0	1333	1583	1.06	236		0.2
2hr	1329	1585	1.1	189		0.2
4hr	1328	1585	1.1	188		0.2
6hr	1328	1585	1.2	212		0.2
8hr	1328	1584	1.2	167	2652	0.2
1ml GO 500mg/l + 10 ml Ethanol paper						
Exposure time	D	G	ID/IG	FWHM (D)	2D	I2D/IG
0	1329	1592	1.1	215		0.3
2hr	1329	1602	1.2	144		0.3
4hr	1328	1601	1.1	155		0.3
6hr	1328	1589	1.2	181	2655	0.3
GO 6.2 g/l paper						
Exposure time	D	G	ID/IG	FWHM (D)	2D	I2D/IG
0	1322	1581	1.09	225		
2hr	1324	1581	1.1	244		
4hr	1320	1580	1.1	446		
6hr	1323	1585	1.09	340		
1ml GO 6.2g/l +35ml Ethanol paper						
Exposure time	D	G	ID/IG	FWHM (D)	2D	I2D/IG
0	1338	1603	1.05	216		0.3
2hr	1326	1591	1.1	205	2647	0.3
4hr	1319	1595	1.2	156	2636	0.3
6hr	1321	1598	1.1	150	2646	0.2

Figure 8-2 shows the Raman spectrum of fabricated GO film using the technique of vacuumed filtration for both diluted and undiluted LC and HC GO films before and after UV–light treatment at different exposure times in the ranging from 2hrs to 6hrs. The presence of epoxy (C-O-C), carboxyl (-COOH), hydroxyl (-OH), and carbonyil (C=O) resulted in D band being recorded in the range of 1391cm^{-1} to 1338cm^{-1} as shown in Figure 8-2. The G band was recorded in the range of 1571cm^{-1} to 1603cm^{-1}. The 2D band was recorded in the range of 2615cm^{-1} to2669 cm^{-1} which is due to the graphene formation after UV treatment. It was found that by increasing the exposure time from 2hrs to 6hrs, the D band intensity was increased, whereas the FWHM of the D band become narrower by increasing the UV light exposure time.

Figure 8-2(a) shows the Raman spectrum of the LC GO paper. This figure shows that although there was not any significant change in 2D band intensity after 6hrs UV exposure, the intensity of 2D band was formed after 8hrs UV treatment in wavenumber of 2652cm^{-1}. In addition, no significant shifts were found in the D and G band positions, which could be attributed to the lower level of reduction in the LC GO paper. Similarly, the intensity of I2D/IG, which is related to the number of layers, was stable at 0.2 before and after 8hrs UV treatment. However, FWHM of D band showed a narrowing of D band from 236cm^{-1} to 167cm^{-1}, which indicates a successful slow reduction.

The recorded Raman spectrum of diluted LC GO paper (1:10) at different UV exposure times was shown in Figure 8-2(b). As can be seen from this figure, the 2D band at a wavenumber of 1655cm^{-1} was recorded after 6hrs UV exposure. It was also found that by increasing the

exposure time from 2hrs to 6hrs, the ID/IG ratio was increased by 1.2 without any significant changes in the D and G band positions. Moreover, the FWHM of the D band was decreased from 215cm^{-1} to 181cm^{-1} after 6hrs exposure, which could be due to the removal of oxygen functional group [32].

The recorderd Raman spectrum of HC GO paper at different UV exposure times is shown in Figure 8-2(c). As can be seen in Table 8-1, there were no significant shifts in D,G position after 6hrs exposure. Therefore, FWHM, of D band showed an increase broadening from 225cm^{-1} to 340cm^{-1}, which indicates an increased defect in the materials without formation of graphene .

In contrast, Raman spectrum from HC GO diluted with 35ml ethanol in Figure 8-2(d), indicates formation of 2D band after 2hurs exposure in wavenumber of 2647cm^{-1}. Further increase of exposure time from 2hrs to 6hrs caused a decrease in FWHM of D band from 216cm^{-1} to 150cm^{-1}. The D band shifted toward a smaller wavenumber from 1338cm $^{-1}$ to 1321cm^{-1}, which indicates successful reduction.

8.3.2 SEM characterization

The surface morphology of fabricated diluted and undiluted LC and HC GO films by means of vacuum filtration was studied by using SEM. Figure 8-3(a) shows a strong conjugation between the undiluted LC GO films before UV light exposure. As can be seen from this figure, the film surface is more uniform without any porous structure compared to the film surface structure after 8hrs exposure (see Figure8-3 [b]) which could be considered defects.

The increase in defect structure as a result of UV treatment can be confirmed by the recording of large intensity D band in the Raman spectrum.

Figure 8-3 (c-d), depicts the SEM image of diluted LC GO films both before (Figure 8-3[c]) and after UV exposure (Figure8-3[d]). As can be seen in Figure 8-3(c), the filtered films contain flakes with weak conjugation. The flake sizes were reduced after 6hrs UV exposure, as shown in Figure 8-3(d).

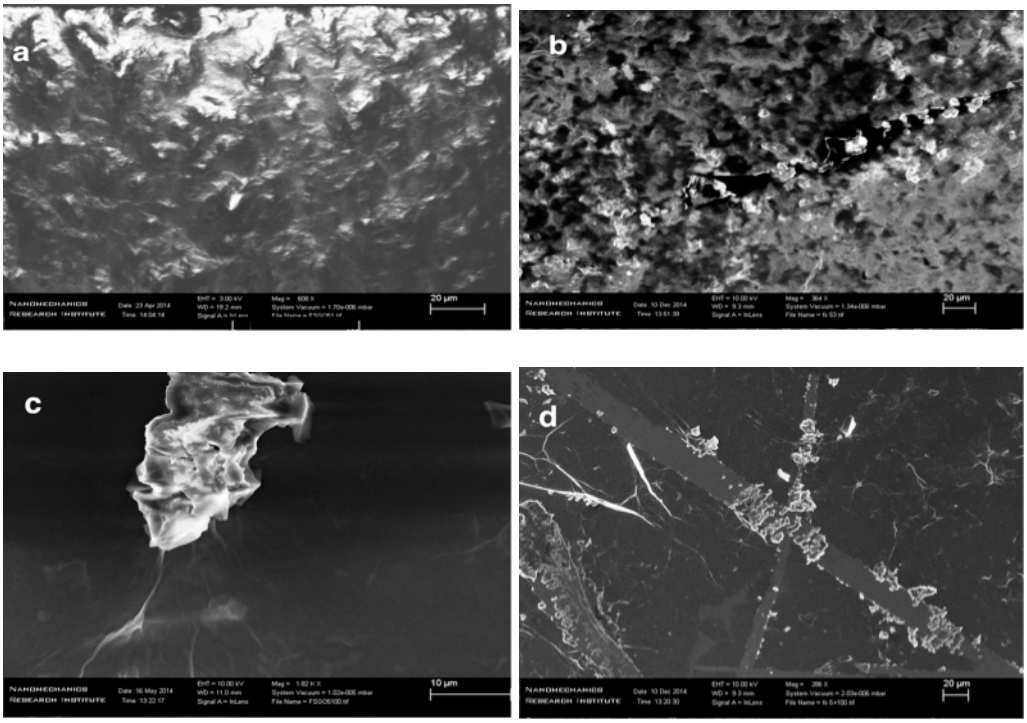

Figure 8-3: SEM image of LC GO film fabricated by means of vacuum filtration of undiluted (a) before and (b) after UV exposure; and diluted (1ml GO: 10ml ethanol) LC GO films (c) before and (d) after UV exposure

Figure 8-4 shows the SEM images of undiluted and diluted HC GO films that were grown by using filtration before and after UV exposure. As can be seen from Figure 8-4(a), a strong stack of layers is observed in the undiluted HC GO films before UV exposure. After 6hrs exposure, GO flakes were separated into small flakes with more conductivity and less thickness, as observed by brighter GO flakes in Figure 8-4(b).

The SEM images of diluted (1ml GO:35ml ethanol) HC GO films before and after UV treatment are shown in Figure 8-4(c-d). As can be seen from Figure 8-4(c), a more coherent and condensed HC GO film was fabricated relative to the film that was fabricated without diluting with ethanol Figure 8-4(a) before UV treatment. As can be seen in Figure 8-4 (d), the GO flakes were broken into smaller GO flakes after 6hrs UV exposure.

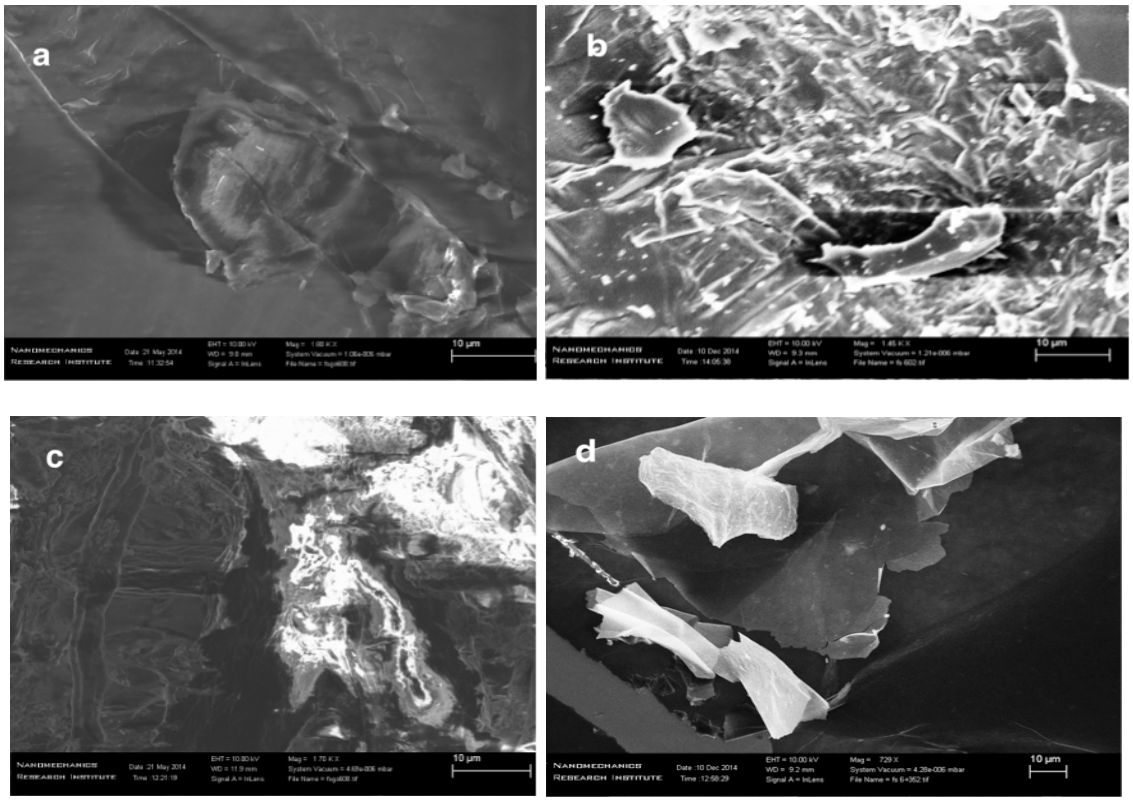

Figure 8-4: The SEM image of HC GO film fabricated by means of vacuum filtration of undiluted (a) before and (b) after UV exposure; and diluted (1ml GO: 35ml ethanol) HC GO film (C) before and (d) after UV exposure

8.4 Conclusion

Applying reduction in graphene oxide membrane instead of film can be appropriate for certain applications. For example, graphene oxide membranes are widely used in gas separation and water purification [33]. In this experimental, I study the effects of UV-treatment on GO membrane chemical composition. Graphene oxide paper is made from HC/LC GO solution via vacuum filtration and baked at 50^{o}C for 6hrs. Next, the film is etched in HCL solution and transferred to silicon substrate. Raman spectrum in general shows slow reduction process after UV treatment compared with GO films prepared via spin coat technique. Undiluted and diluted low concentration GO paper formed graphene after 8hrs and 6hrs, respectively. Furthermore, G and D band position did not change significantly during UV-treatment. The intensity of D band increased after each exposure time, which indicated formation of defect. In contrast, high concentration undiluted graphene oxide paper did not show any structure modification after exposure to 6hrs UV expossure. Diluted HC GO membrane formed after 6hrs UV treatment. In terms of surface morphology, SEM image from undiluted HC/LC GO showed a strong stacking layer due to the removable of water molecules during filtration and baking. In contrast, diluted HC/LC GO paper showed less GO stacking layer.

Chapter 9: Conclusion and Future Research

In conclusion, this work focuses on fabricating reduced graphene oxide using three methods: annealing at low temperature, mixing graphene oxide solution with ethanol, and finally exposure to UV-light. This method can be enhanced in future work by improving reduction mechanism. For example, in terms of annealing at low temperature, increasing the annealed time to 1hr at 90^{o}C could result in formation of graphene. Moreover, modifying graphene oxide solution before fabricating the film with other alcohol components could result in better performance. Finally, using laser instead of UV-light could show a faster reduction process.

Bibliography

1. Eigler, S. and A. Hirsch, *Chemistry with graphene and graphene oxide-challenges for synthetic chemists.* Angew Chem Int Ed Engl, 2014. **53**(30): p. 7720-38.
2. Novoselov, K.S., et al., *A roadmap for graphene.* Nature, 2012. **490**(7419): p. 192-200.
3. Wan, X., Y. Huang, and Y. Chen, *Focusing on Energy and Optoelectronic Applications: A Journey for Graphene and Graphene Oxide at Large Scale.* Accounts of Chemical Research, 2012. **45**(4): p. 598-607.
4. Compton, O.C. and S.T. Nguyen, *Graphene Oxide, Highly Reduced Graphene Oxide, and Graphene: Versatile Building Blocks for Carbon-Based Materials.* Small, 2010. **6**(6): p. 711-723.
5. Pei, S. and H.-M. Cheng, *The reduction of graphene oxide.* Carbon, 2012. **50**(9): p. 3210-3228.
6. Lazauskas, A., et al., *Thermally-driven structural changes of graphene oxide multilayer films deposited on glass substrate.* Superlattices and Microstructures, 2014. **75**(0): p. 461-467.
7. Ding, Y.H., et al., *A green approach to the synthesis of reduced graphene oxide nanosheets under UV irradiation.* Nanotechnology, 2011. **22**(21): p. 215601.
8. Kumar, P., et al., *Novel Radiation-Induced Properties of Graphene and Related Materials.* Macromolecular Chemistry and Physics, 2012. **213**(10-11): p. 1146-1163.
9. Dreyer, D.R., R.S. Ruoff, and C.W. Bielawski, *From Conception to Realization: An Historial Account of Graphene and Some Perspectives for Its Future.* Angewandte Chemie International Edition, 2010. **49**(49): p. 9336-9344.
10. Zhu, Y., et al., *Graphene and graphene oxide: synthesis, properties, and applications.* Adv Mater, 2010. **22**(35): p. 3906-24.
11. Edwards, R.S. and K.S. Coleman, *Graphene synthesis: relationship to applications.* Nanoscale, 2013. **5**(1): p. 38-51.
12. Ferrari, A.C., *Raman spectroscopy of graphene and graphite: Disorder, electron–phonon coupling, doping and nonadiabatic effects.* Solid State Communications, 2007. **143**(1–2): p. 47-57.
13. Ferrari, A.C. and D.M. Basko, *Raman spectroscopy as a versatile tool for studying the properties of graphene.* Nat Nano, 2013. **8**(4): p. 235-246.
14. A.K.Sood, C.N.R.R.a., *Graphene synthesis, properties, and phenomena*. 2013: WILEY-VCH.
15. Konios, D., et al., *Dispersion behaviour of graphene oxide and reduced graphene oxide.* J Colloid Interface Sci, 2014. **430**: p. 108-12.
16. Jalili, N. and K. Laxminarayana, *A review of atomic force microscopy imaging systems: application to molecular metrology and biological sciences.* Mechatronics, 2004. **14**(8): p. 907-945.
17. Zhou, W., et al., *Fundamentals of Scanning Electron Microscopy (SEM)*, in *Scanning Microscopy for Nanotechnology*, W. Zhou and Z. Wang, Editors. 2007, Springer New York. p. 1-40.

18. Zhang, B., et al., *Radiation induced reduction: an effective and clean route to synthesize functionalized graphene.* Journal of Materials Chemistry, 2012. **22**(16): p. 7775-7781.
19. *How an FTIR Spectrometer Operates*. Available from: http://chemwiki.ucdavis.edu/Physical_Chemistry/Spectroscopy/Vibrational_Spectroscopy/Infrared_Spectroscopy/How_an_FTIR_Spectrometer_Operates.
20. Norimatsu, W. and M. Kusunoki, *Epitaxial graphene on SiC{0001}: advances and perspectives.* Physical Chemistry Chemical Physics, 2014. **16**(8): p. 3501-3511.
21. Zhang, Y., L. Zhang, and C. Zhou, *Review of Chemical Vapor Deposition of Graphene and Related Applications.* Accounts of Chemical Research, 2013. **46**(10): p. 2329-2339.
22. Jayasena, B. and S. Subbiah, *A novel mechanical cleavage method for synthesizing few-layer graphenes.* Nanoscale Res Lett, 2011. **6**(1): p. 95.
23. Su, C.-Y., et al., *High-Quality Thin Graphene Films from Fast Electrochemical Exfoliation.* ACS Nano, 2011. **5**(3): p. 2332-2339.
24. Huang, L., et al., *Pulsed laser assisted reduction of graphene oxide.* Carbon, 2011. **49**(7): p. 2431-2436.
25. Gong, C., et al., *Graphitization of Graphene Oxide with Ethanol during Thermal Reduction.* The Journal of Physical Chemistry C, 2012. **116**(18): p. 9969-9979.
26. Eigler, S., C. Dotzer, and A. Hirsch, *Visualization of defect densities in reduced graphene oxide.* Carbon, 2012. **50**(10): p. 3666-3673.
27. Lin, Y., J. Jin, and M. Song, *Preparation and characterisation of covalent polymer functionalized graphene oxide.* Journal of Materials Chemistry, 2011. **21**(10): p. 3455-3461.
28. Chang, H.-W., et al., *Reduction of graphene oxide in aqueous solution by femtosecond laser and its effect on electroanalysis.* Electrochemistry Communications, 2012. **23**(0): p. 37-40.
29. Kudin, K.N., et al., *Raman spectra of graphite oxide and functionalized graphene sheets.* Nano Lett, 2008. **8**(1): p. 36-41.
30. Eda, G., G. Fanchini, and M. Chhowalla, *Large-area ultrathin films of reduced graphene oxide as a transparent and flexible electronic material.* Nat Nano, 2008. **3**(5): p. 270-274.
31. Chen, J., et al., *Controllable fabrication of ultrathin free-standing graphene films.* Philosophical Transactions of the Royal Society of London A: Mathematical, Physical and Engineering Sciences, 2014. **372**(2013).
32. Diez-Betriu, X., et al., *Raman spectroscopy for the study of reduction mechanisms and optimization of conductivity in graphene oxide thin films.* Journal of Materials Chemistry C, 2013. **1**(41): p. 6905-6912.
33. Tang, Y.P., D.R. Paul, and T.S. Chung, *Free-standing graphene oxide thin films assembled by a pressurized ultrafiltration method for dehydration of ethanol.* Journal of Membrane Science, 2014. **458**(0): p. 199-208.